Instrument Characterization and Calibration for Altimira Observatory (G76)

Contents:

1. Purpose: This report documents the characterization and calibration of the Altimira Observatory instruments, conducted initially during August-September 2003, and augmented sporadically thereafter.

The instrument package consists of: Celestron NexStar-11 telescope with Agos focal reducer operating at nominal f/6.3, SBIG CFW-8A filter wheel with photometric B, V, and R filters, and SBIG ST-8XE CCD imager.

2. Summary of Results: Following are key notes drawn from these characterization experiments:

- The linear range of the imager is from 1,000 ADU to 50,000 ADU (after dark-correction).
- Flat-field images should strive for peak pixel signal of about 35,000 ADU
- "Drum" lightbox provides flat-fields that are flat to less than 1% residual error.
- Filter wheel position non-repeatability generates flat-field errors of about 1% to 2% peak-to-peak)
- desired focus accuracy of ± .002 inch corresponds to ± 1 second of focus motor motion at "dead slow"

3. Field of view:

3.1 Reticle eyepiece: The reticle dimension of my Meade 12 mm reticle eyepiece was measured by stop-watch timing of the transit of a star across the reticle. (The star was at the celestial equator, where the siderial rate is 15 arc-sec per second. Transit time across the reticle's two lines was 1.01 ± .08 sec, indicating that the reticle line spacing is ≈ 15 ± 1 arc-sec, as illustrated below:

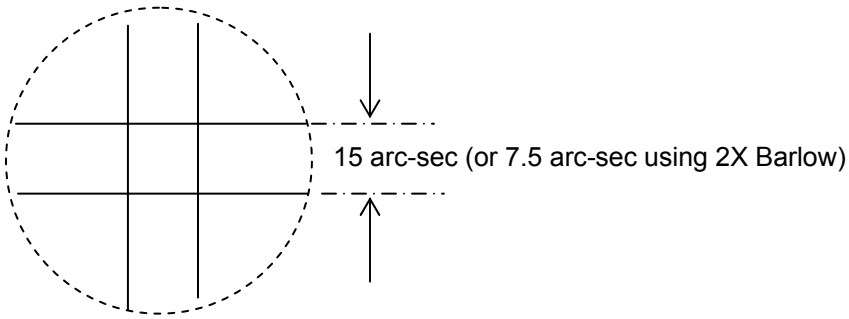

3.2. Image orientation: Different software packages display the image somewhat differently. With the CCD oriented as shown in the sketches below:

- CCDSoft screen display of images during imaging operations is:

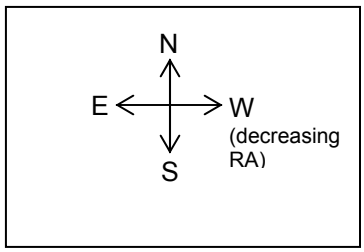

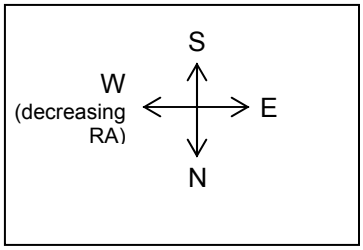

Saved files displayed in CCDSoft have the same orientation.

The image/file orientations for use in other programs is dexcribed in the table below:

	“cables down” orientation	**“cables up” orientation**
SkyMap Pro charts	Match the “cables down” orientation without any flipping or rotation.	Must be “flipped” E-W and N-S to match the “cables up” orientation.
AstroArt	Saved images imported into AstroArt are flipped vertically in the “cables down” orientation – in order to match SkyMapPro charts, either the image or the chart must be flipped (north for south).	Saved images imported into AstroArt are flipped horizontally.
MPO Canopus	Displays these images in the correct orientation to match the star catalog without any flipping or rotations.	Check the “flip N-S” and “flip E-W” boxes to match the star catalog orientation.
TheSky charts	North = “up”	North = “down”

3.3 FOV of CCD imager: Per SBIG’s data sheet, the main imager FOV is 27 arc min X 18 arc min. The Guide chip FOV is 9.6 arc min X 7.3 arc min.

The main imaging chip’s pixel size is IFOV= 1.1 arc sec (square), for 9 μm pixels. The tracking chip IFOV is a bit smaller (7.4 μm pixels).

The relative orientation of these FOV’s is illustrated below. For the “cables down” camera orientation, the guide chip is North of the imaging chip. For the “cables up” orientation, the guide chip is South of the imaging chip.

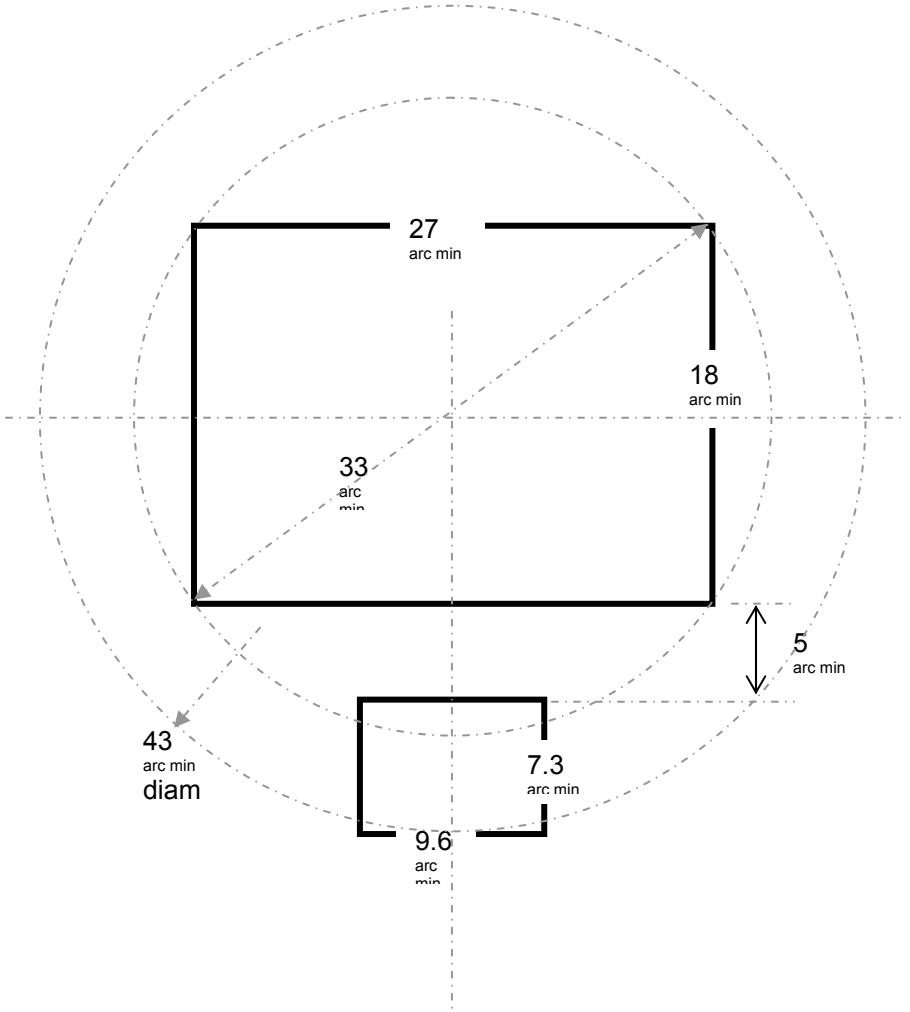

4. Linearity: Photometric measurements depend on the accurate linearity of the CCD imager's response. This series of measurements validated the linearity of the ST-8XE, and defined the upper and lower signal levels of the linear regime.

4.1 Signal Linearity: Several images of the field of NGC 6926 were taken at different exposure duration, and dark-subtracted and flat-field corrected. A perfectly linear sensor would show S ~ Δt (i.e. integrated signal proportional to exposure time) – straight lines of slope= 1.0 on a plot of log S vs. log Δt. Figure 1 shows the field selected for this test, and the 5 stars that were used.

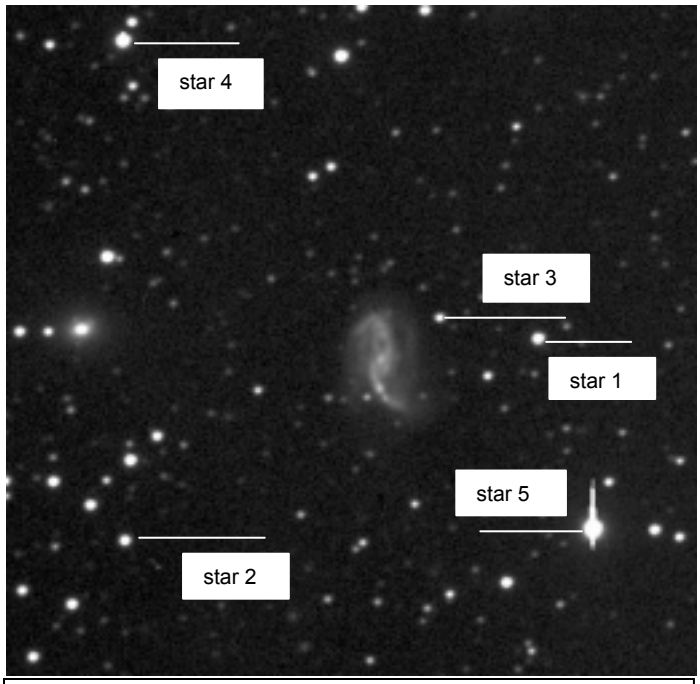

Figure 1: Field & stars used for linearity check

Figure 2 shows the resulting integrated signal for these stars vs. exposure duration. Note that all stars display a very linear response, except (at the maximum signal) for Star 5, which shows the effect of saturating the CCD's charge wells; and (at the minimum signal) for Star 3, which seems to show a slight drop in signal (perhaps due to sky background interference?). Leaving a little safety room at these upper and lower signal limits, the imager can be considered to be linear over the range of S_{min}= 10,000 ADU to S_{max}= 2,500,000 ADU.

Note that two exposures each were made for the 60-second and 240-second data points. This provides an indication of the (very good) consistency of different exposures. Also, the two 60-second exposures were taken at the beginning and the ending of this imaging sequence, to confirm that sky conditions did not change noticeably during this test.

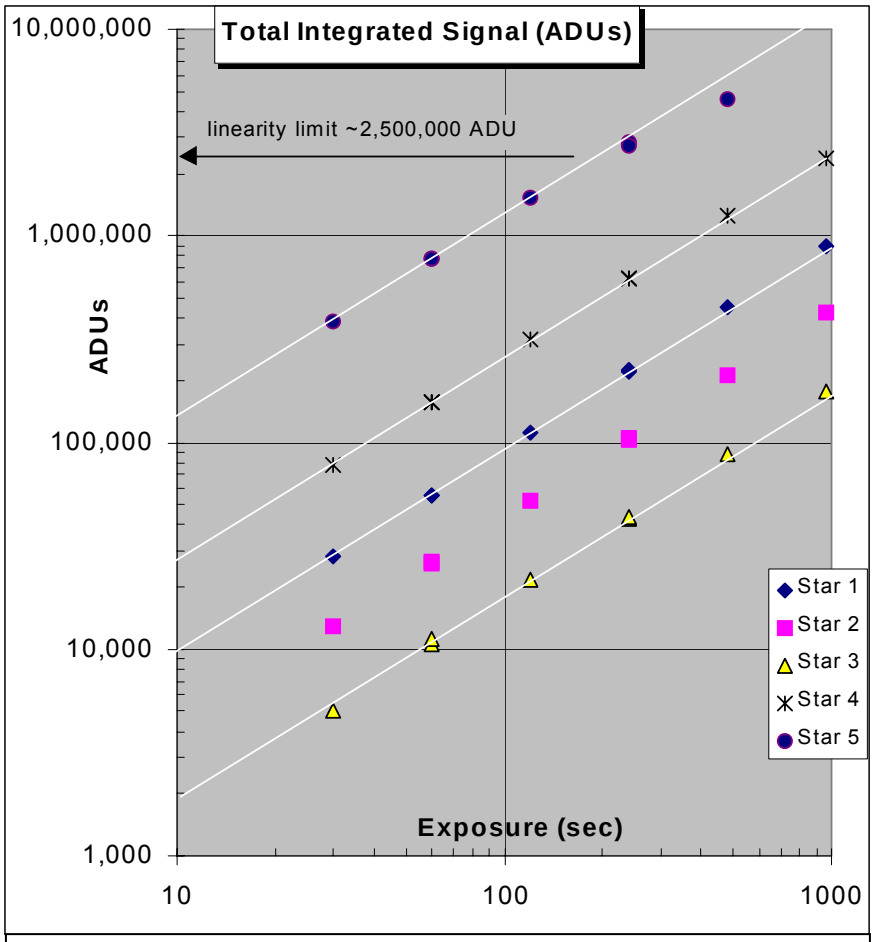

Figure 2: Linearity of Integrated Signal for stellar images is excellent between 10 X 10^3 and 2.5 X 10^6 ADUs

The peak signal of a stellar image should also be very nearly linear with exposure duration, but there will be more scatter in the data because the exact peak of the star's point-spread-function may fall exactly on the center of a pixel (maximizing the "peak signal" response), or it may fall between two pixels (reducing the "peak signal" response because the peak is shared between two pixels). Figure 3 shows the peak-signal response of the same data set:

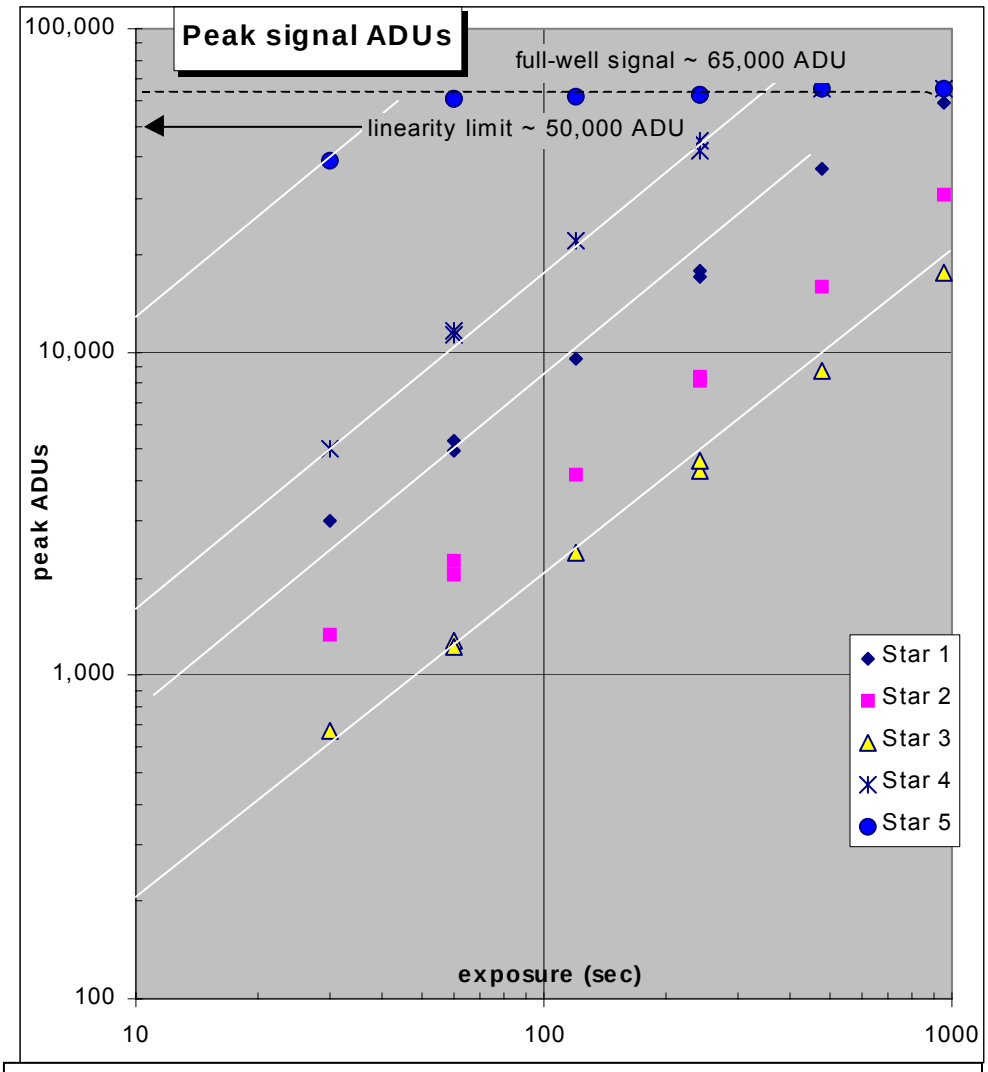

Figure 3: Peak-pixel signal for stellar images is linear between 1,000 ADU and 50,000 ADU

The full-well capacity of the ST-8XE (non-anti-blooming) chip is about 65,000 ADU. The effect of saturation of the wells can be seen in the curve for Star 5 (the brightest star, which is noticeably saturated in the image of Figure 1). Again leaving a little safety room, the peak signal is nicely linear from signal levels of 1,000 ADU (see the 30-sec exposure of Star 3) to 50,000 ADU.

These results are useful both for (a) selecting appropriate exposure duration for photometric studies, and (b) setting exposure/signal level for flat-fields.

Photometric studies should be set up so that both the target object and the comparison stars fall in the range 10,000 to 2,500,000 integrated ADUs, and peak pixel falls in the range 1,000 to 50,000 ADU.

Flat-field images should strive for pixel signal of about 35,000 ADU per pixel, and never more than 50,000 ADU per pixel.

4.2 Dark-Frame characteristics: The dark-frame pixel value theoretically contains two effects: (a) read-out noise that is constant, independent of exposure; and (b) thermal-noise that accumulates and hence should increase with exposure duration, and also increase with chip temperature.

A series of dark-frames were made, all at chip temperature T=0 °C, to investigate the dark-frame vs exposure characteristics. Since each pixel has slightly different gain, and there are a (small) population of "hot pixels" whose dark-current is noticeably higher than the average pixel, the dark-frame ADUs are described statistically. Both AstroArt and CCDOps calculate the average pixel (and both give the same value for any given image, happily); AstroArt also calculates the standard deviation, and the max and min pixel values; and CCDOps also calculates the 1st percentile, median (50th percentile) and 99th percentile values of the image histogram. Examination of the histograms shows that each dark-frame's ADUs are (roughly) normally distributed – a bell-curve with a very low-level, long tail out to the high ADU values.

The dark-frame ADU statistics are illustrated below:

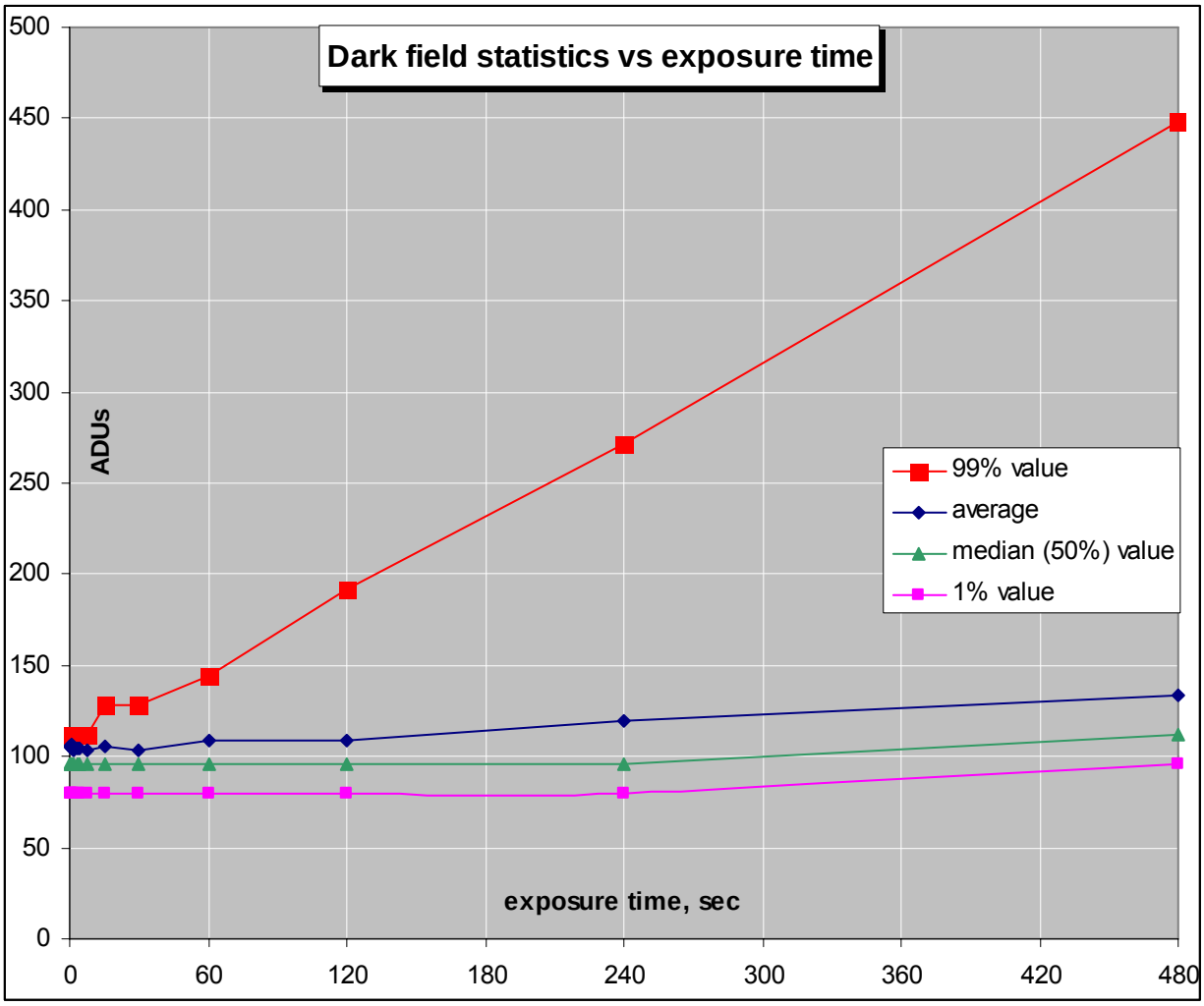

The best linear fit to the 99th percentile curve is:

$$99^{th} \text{ percentile ADUs} = 109.51 + 0.6976\ \Delta t$$

where Δt is the exposure, in seconds. I haven't seen any guidance on the subject of maximum exposure length, but I suspect that it is undesirable to use more than about 10% of the dynamic range for thermal noise – i.e. the 99th percentile ADUs should be kept to below about 6000 ADU.

Using this criterion, the longest practical single exposure is $\Delta t_{max} \approx 120$ minutes = 2 hours. This doesn't sound like a serious restriction!

The "hot pixels" comprise a very small fraction of the total image, and are generally fairly widely scattered, so I'll ignore their unusual contribution. I note, however, that once a hot-pixel becomes saturated, it's probably impossible to get reliable information from that pixel on the image, and hence it may distort photometry somewhat. The "max pixel" value vs dark field exposure (again, at T= 0 °C) is shown in the graph below:

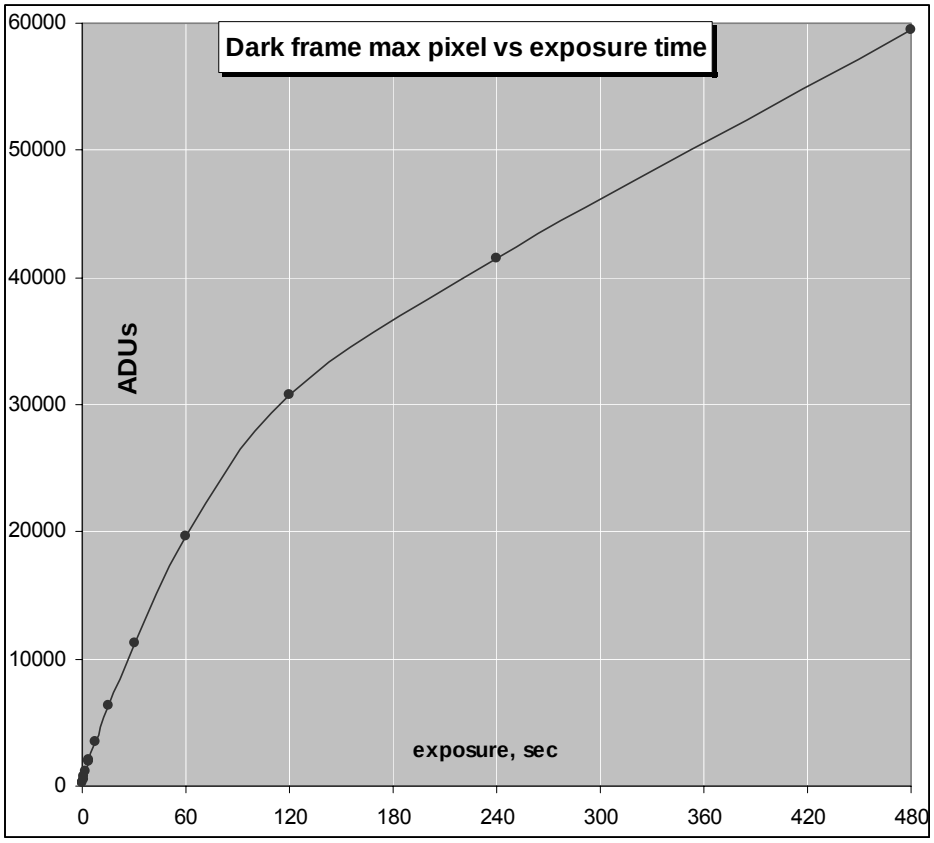

The identity of the "hottest" pixel varies from frame to frame (probably due to the effect of noise on top of the pixels' gain variation.

5. Vignetting & Uniformity: It is of interest to know how much vignetting or chip non-uniformity exists in the uncorrected image, as a means of assessing the importance of flat-field correction of photometric images. Separate flat-fields will be needed for each filter used. It is also of interest to assess the "flatness" of the flat-field source – I'll do this be comparing two different "dome-flats" taken with different lighting conditions, and a "twilight flat"

5.1 Unfiltered Uniformity: A typical dome-flat (unfiltered image), dark-corrected, is shown in Figure 2 below. Note the shading (particularly pronounced on the left edge and lower corners) that is probably a result of vignetting in the optical train, and the dust donuts scattered over the image. The large dust donuts (such as the prounounced one at the center of the image) come from optical surfaces relatively far from the imager – probably the focal reducer lens. The tiny dust donuts come from an optical surface closer to the imager – probably the cover-glass in front of the CCD. (This is an unfiltered image: on B, V, or R images some intermediate-size donuts arising from dust on the filter glass are also expected).

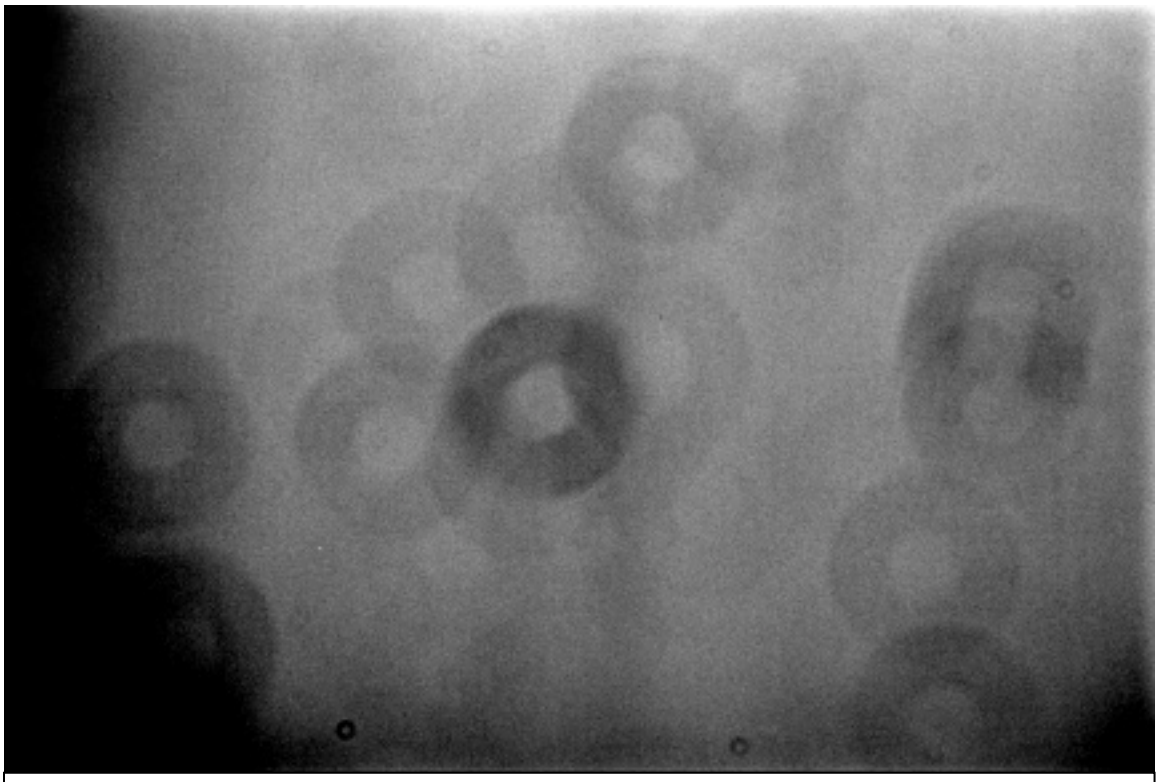

Figure 4: Typical flat-field ("dome flat") image after dark-correction.

The intensity of these defects is greatly enhanced in the Figure above, by displaying only a tiny portion of the intensity range in the raw image. In order to assess the magnitude of these defects, and their effect on photometric studies, an intensity profile was made diagonally across this image (from upper left to lower right).

The pixel signals on this profile are plotted in Figure 3 below. The little dots are the pixel-by-pixel signal (in ADUs), and the white curve shows the 11-point moving average of the pixel values. These two pieces of information show two things:

The white (11-point moving average) curve illustrates the gross shading and dust donuts.

The overall shading shows up as the reduced intensity at the left and right edges of the graph. The total shading across this flat field is about 3500 ADUs, amounting to about

3500/36,000 ≈ 10%. If the vignetting in the corners is excluded (i.e. keep the photometric target in the central half of the FOV), then the shading – mostly due to dust donuts – is about 500 ADU ≈ 500/36,000 ≈ 1.5% below the general trend.

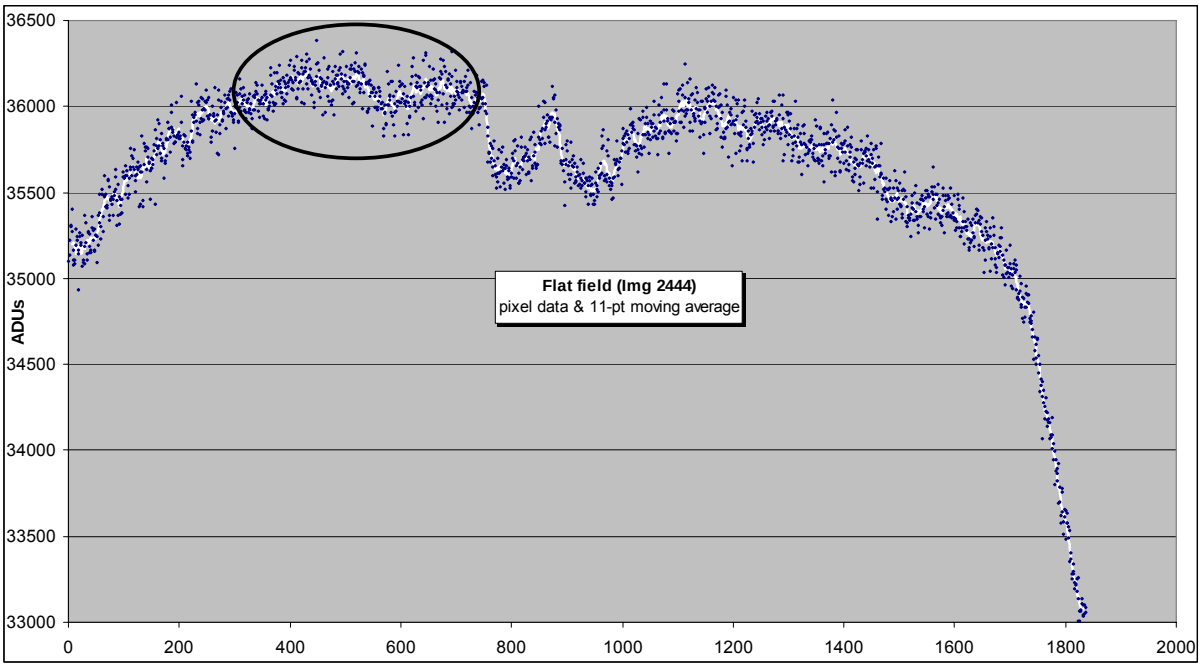

The scatter of the individual data points (above and below the trend-line) give an indication of the variation in individual pixels' response to essentially identical light input. This scatter is illustrated by expanding a small portion of the profile, which is shown in Figure 4. Calling the individual pixel signal S(x), and the 11-point moving average Avg(x), then statistical

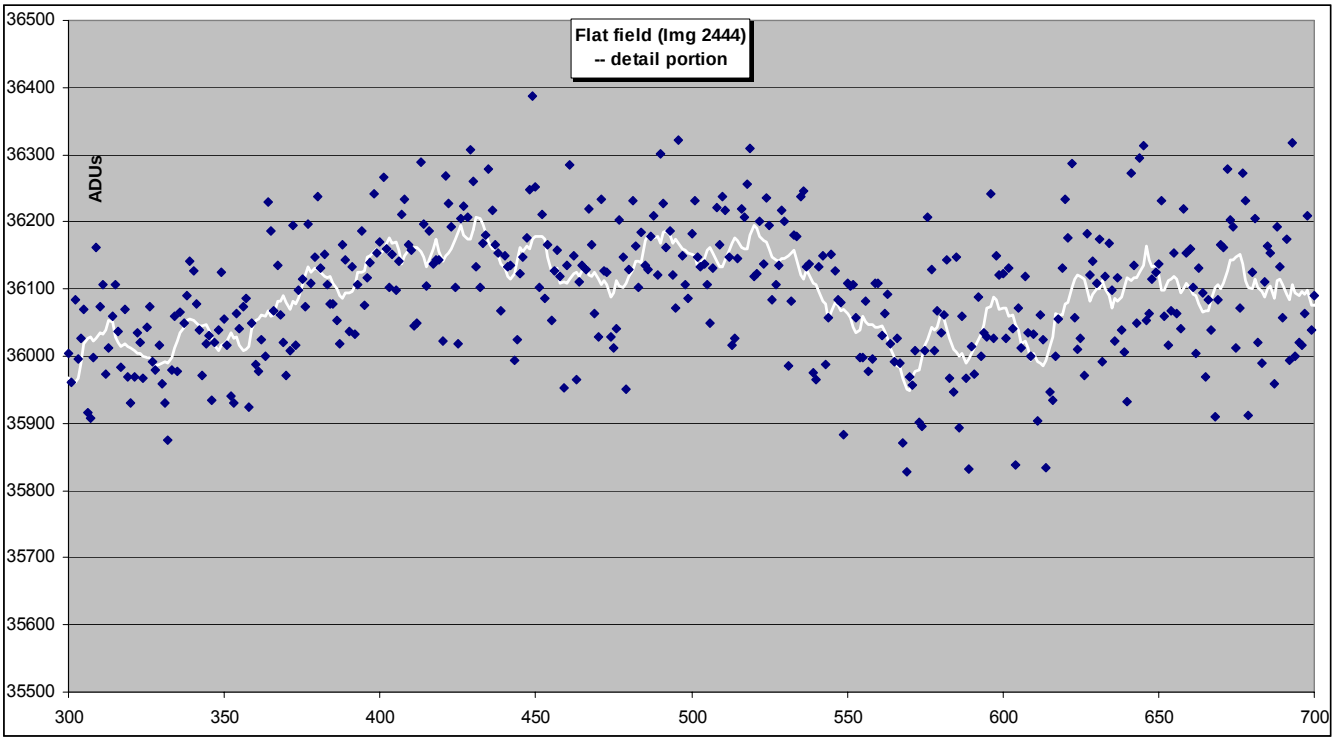

analysis of S(x) – Avg(x) gives:

mean= -.015

(i.e. essentially zero – the white curve is a good representation of average light intensity on small groups of pixels), and

std deviation= 79.4

(i.e. the 1-σ pixel-to-pixel variation in sensitivity is about $\pm$0.2%).

These results illustrate that accurate flat-fielding is needed in order to get photometric accuracy better than about 3%; but that also the accuracy of the flat-field must be very good (i.e. better than 3%) in order for it to be beneficial.

5.2 "Flatness" of Dome Flats: In order to assess the flatness and consistency of the "dome-flat" method, I took three dome-flats, and a couple of twilight-flats. The Dome flats are taken using the SBIG-recommended method, of having a flashlight reflect off a diffuse white surface onto a second diffuse surface (a grey foam-board circle mounted to the dome), and then into the telescope.

Figure ___ compares the diagonal-profile pixel intensity for each of these 5 flat-fields:

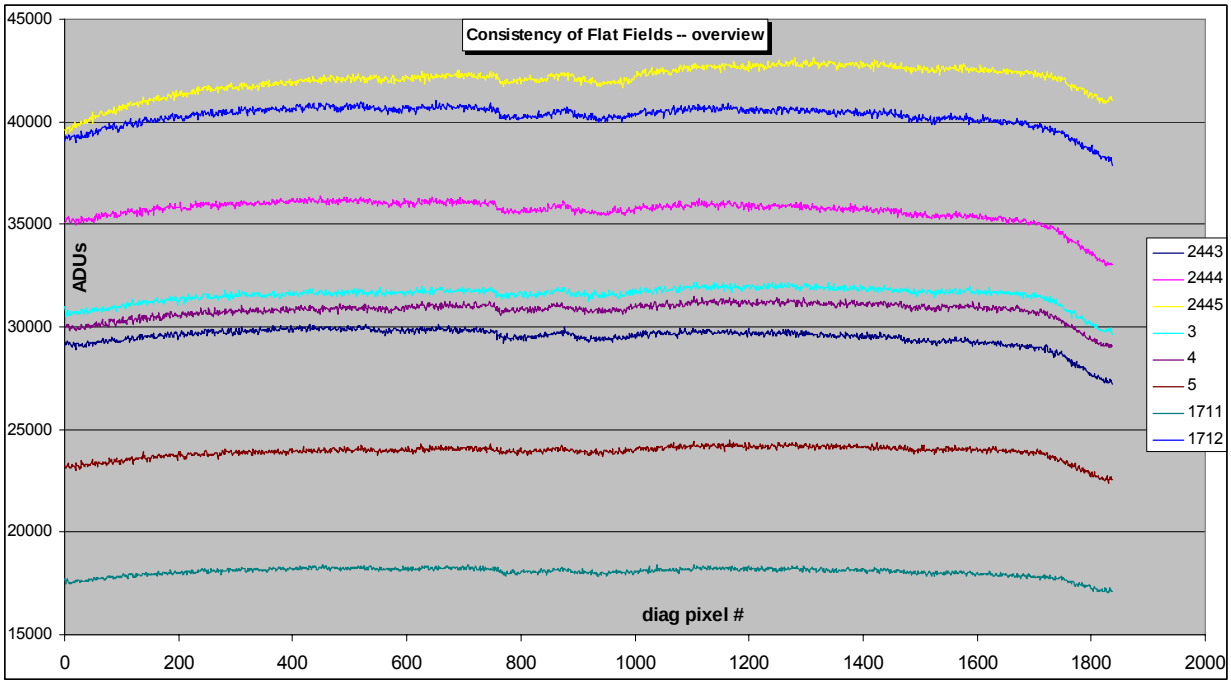

Qualitatively, they appear very similar (aside from the inconsequential differences in overall-intensity caused by different exposure durations), but cose examination shows a few inconsistencies (e.g. see the different slope of image "2445" compared to image "1712" on the right portion of the plots).

The first comparison is the consistency of dome flats – is one dome flat the same as another? The ratio of two pairs of dome flats is shown in Figure ___ below:

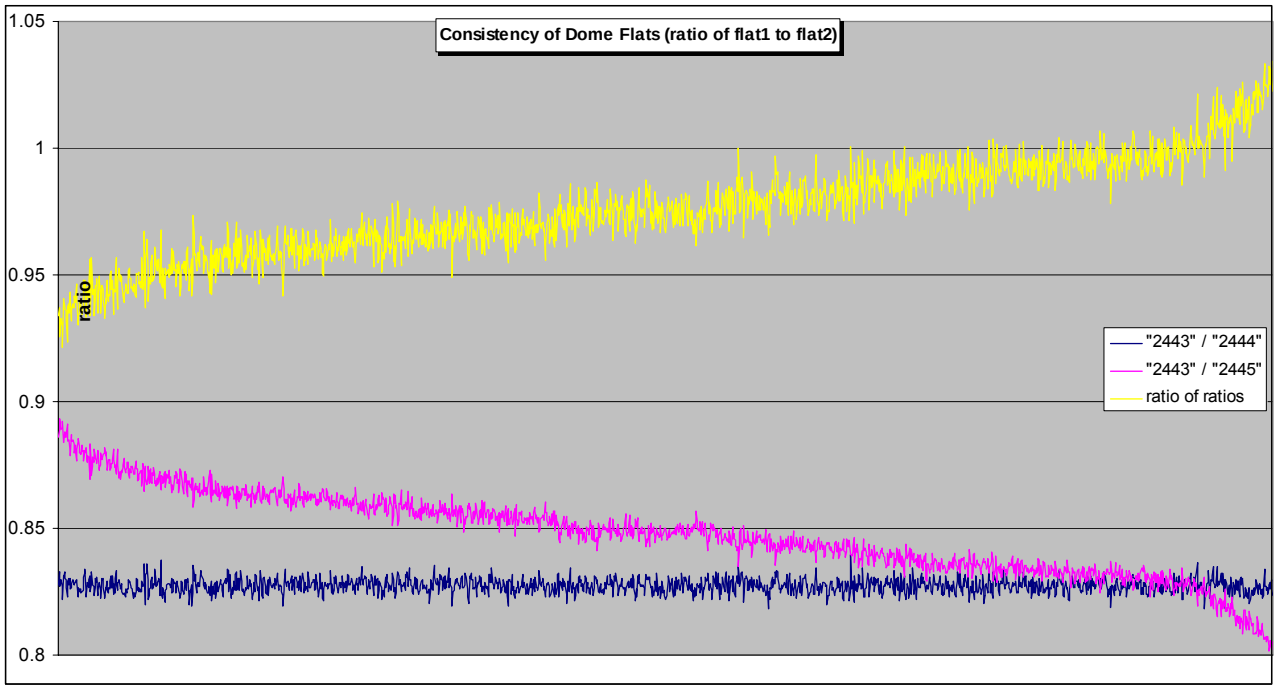

This result is not encouraging – flat "2445", made under essentially the same conditions as flats "2443" and "2444" is clearly different from those two ("2445" was made with the flashlight on the opposite side of the telescope compared to 2443 and 2444). Detailed statistical analysis shows that the RMS ratio error (in the case of "2445") is 1.6%. The curves above show that the method of making dome flats is not sufficiently controlled and consistent: it can give variation of 3% to 10% (peak) in the flat field – equal to or larger than the errors that it is intended to correct!

5.3 "Flatness" of Twilight flats: A set of three twilight flats were made on the same night, for comparison. Figure ___ below shows the consistency of these twilight flats (again based on the ratio of flat-1 to flat-2):

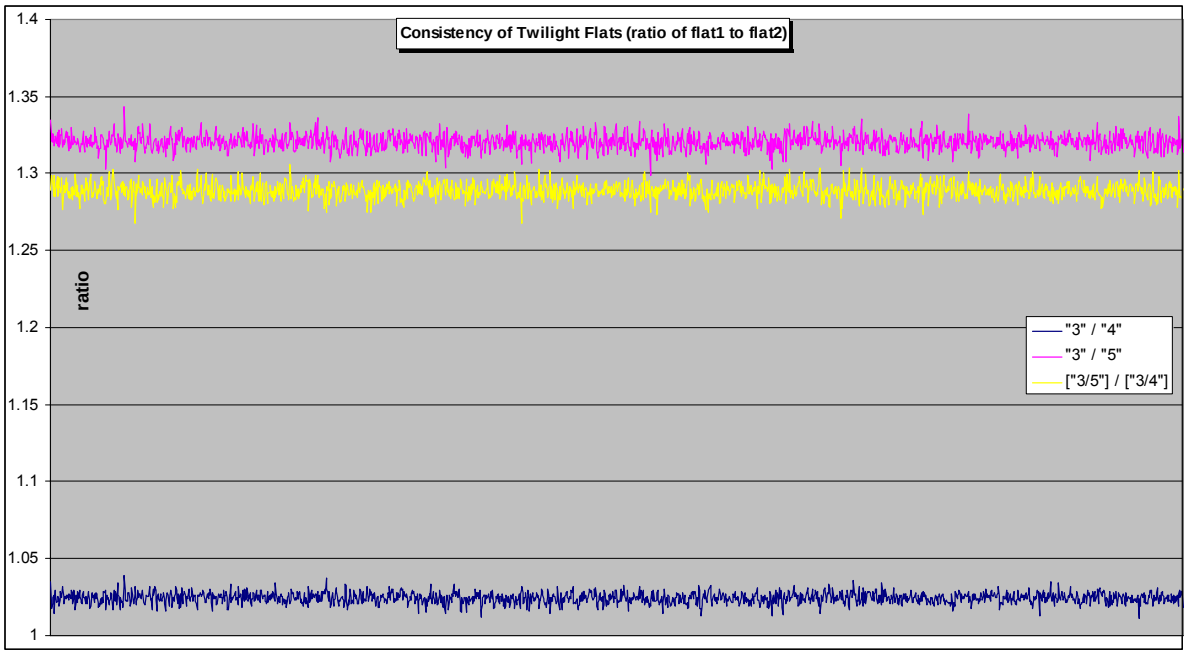

Here, the results are much better. Detailed analysis shows that the standard deviation of the ratio is between 0.3% and 0.5%.

This is why a well-done set of twilight flats is the "gold standard" for flat fielding. They're just not very convenient compared to a dome flat

The relatively poor consistency of "dome flats" prompted the design and fabrication of the "drum" lightbox.

5.4 Light-box flats: Tests of the flatness of Light Box flats (using the "round drum" lightbox), and determination of the required flat-field exposure for the different photometric filters is described below.

Using the 6-volt power supply on the "drum" lightbox with 5 lightbulbs, the following exposures achieve good flat-field signal levels (average about 30,000 to 45,000 ADUs) – high signal, but not saturated:

CCD filter	lightbox reflector	exposure, sec	typical range of ADUs
unfiltered	grey	4	42,975
R (red)	white	5	23,500 – 26,300
V (visible)	white	35	21,000 – 23,300
B (blue)	white	600 (5 min)	19,000 – 24,000

5.4.1 Unfiltered: Two lightbox flat-field exposures were made, then the lightbox was rotated 90 degrees, and two more were taken. The "0 degrees" flats were averaged, and the "90 degrees" flats were averaged, then the the "0 deg avg" and the "90 deg avg" were divided in AstroArt, to determine if any structure remained. The resulting "ratio" image appeared very uniform, aside from noise. Profiles from corner-to-corner also show good uniformity, to the ± 0.5% level, as shown in the graph below:

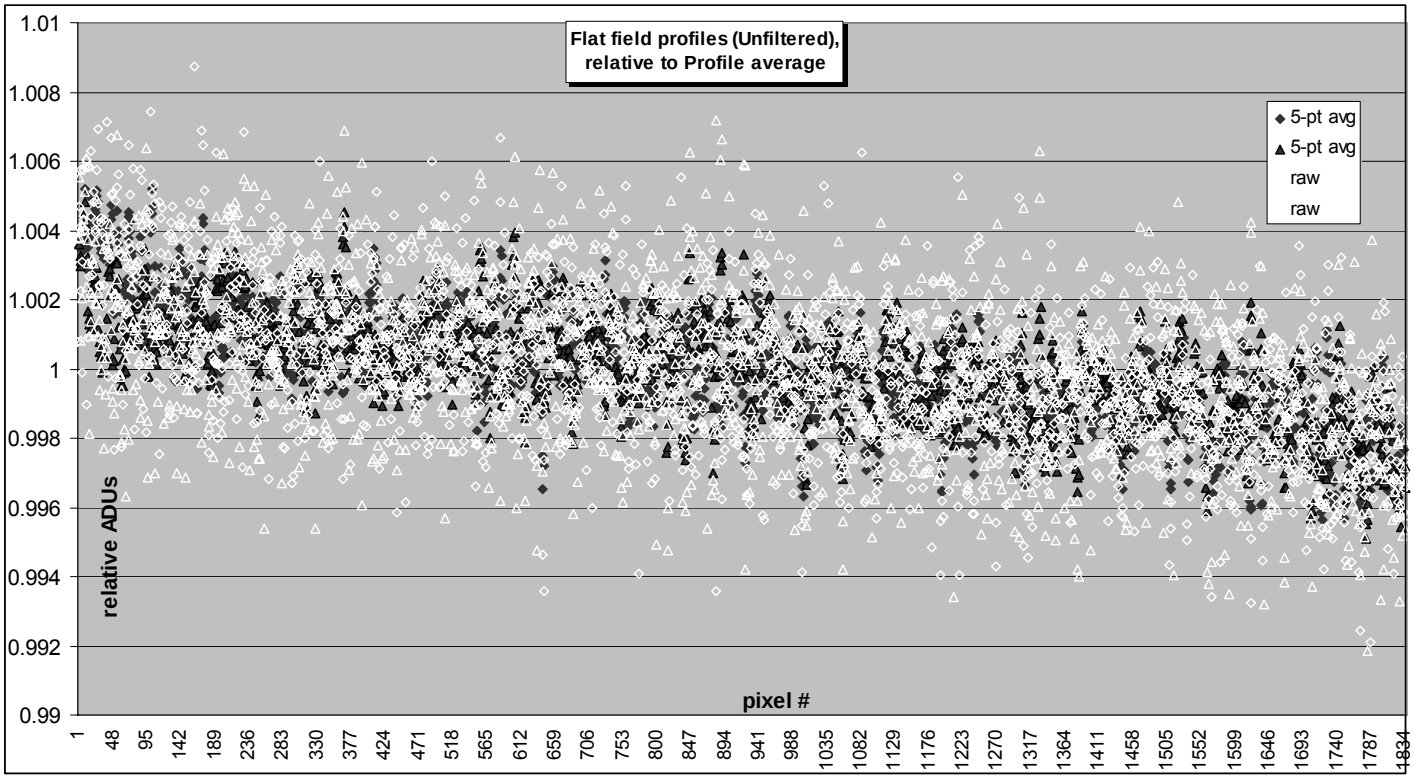

Looking at the "least-constant" profile of the resulting image, and defining the "flatness consistency error" as:

Err = ± (max-min)/(2*avg)

yields an estimated flatness consistency error of ± 0.8% (which will translate directly into an 0.8% photometric error due to this error source – a satisfactory condition)

This indicates that the "drum" lightbox is giving good consistency in flats.

5.4.2 Red filter: A similar exercise using the R-filter flat fields showed that if the "90 degree avg" isused as the flat-field reference to correct the "0 degree avg", then the resulting image is essentially flat and unstructured to the ± 0.5% level. Diagonal profiles of the result are shown below:

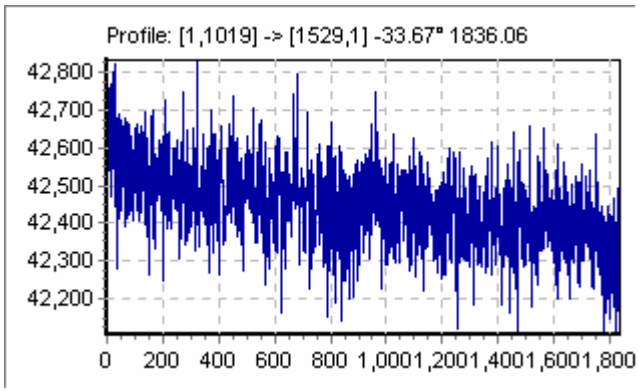

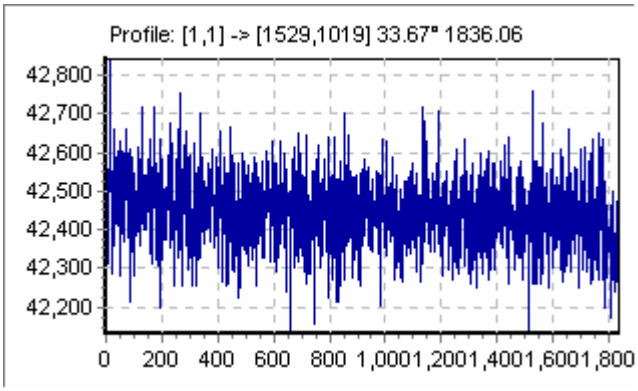

(Arithmetic: peak-to-peak variation is approximately (42,700 – 42,300)/42,500 ≈ 1 %)

As a check, I also used the "unfiltered" flats to correct the "R filter" flat-images, and the results showed two effects: the unique dust-donuts affecting the R-filter are apparent, and some vignetting caused by the filter is also visible, particularly near the corners of the field of view, as shown in the image below:

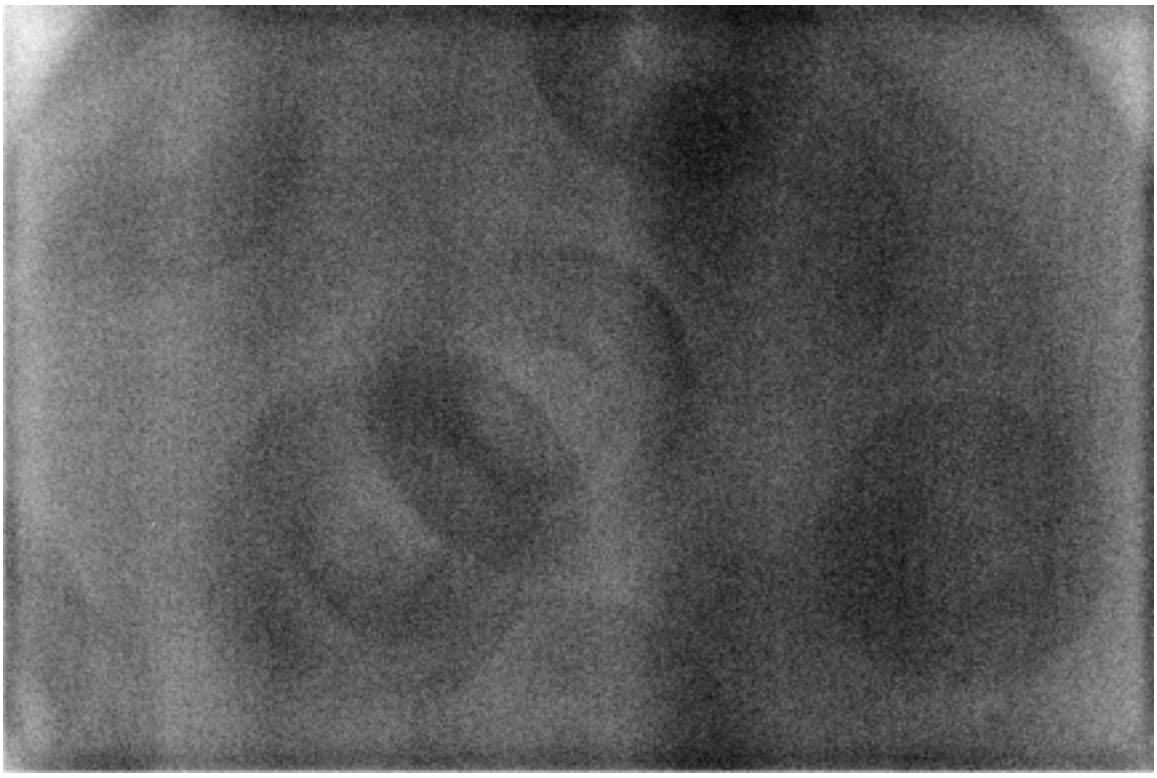

The profile of this image shows that the peak-to-peak variation is about 2% (i.e. the vignetting in the filter wheel adds about a 2% shading in the image; but proper flat-fielding reduceds this to about 0.5% photometry error).

5.4.3 Visible filter: V-band checks gave very similar results to the R-band: similar vignetting compared to the unfiltered image), and "0-degree flat"-to- "90 degree flat" consistency of about 0.5%.

5.4.4 Blue filter: B-filter checks gave similar results – good consistency between flats, but peak-to-peak flatness was about 1.0%.

5.5 Repeatability of Filter Wheel Position:

An experiment was done by taking a set of v-band flat fields, then rotating the filter wheel one complete turn, then taking another set of v-band flat fields. Set #1 was then used as the "flat" to correct Set #2. If the two sets were identical, then a uniform flat screen (with some noise) would result.

The actual result was subtle shadow pattern similar to the raw flat, with a peak-to-peak value of about 1%. This is presumably caused by imperfect reeatability of the filter wheel position – slight position difference are convolved with vignetting and result in an uncorrected pattern.

The implication of this is that for the most critical projects (e.g. transit search, where the accuracy requirement is a fraction of a percent), the filter wheel should not be moved for the duratin of the imaging sequence.

5.6 Guide Chip Vignetting:

Flat fields of the guide chip were also made, as a check of vignetting from the filter wheel with the F/6.3 focal reducer.

There is noticeable vignetting, amounting to over 50% loss of signal in the upper portion of the guide chip. In general, guide stars should be placed in the lower half of the guide chip.

7. Focus Rate: The motion of the JMI NGF-S focuser was measured with a dial-indicator and a stopwatch. The motion rates are:

- "dead slow" = 3 mils/sec = .003 inch /sec
- "max fast" = 6 mils/sec = .006 inch/sec

The backlash in the focus drive creates a dead-band of about 1 second when the direction of motion is changed (i.e. there is no focus motion for the first ~ 1 sec of motor rotation.)

The required focus accuracy to keep the circle of confusion no larger than the 9μm pixels of the image, at f/6.3, is

$\Delta x = \pm 6.3 \cdot (9X\ 10^{-6}) \cdot 39.37$ in/m = ± 0.002 inch

This corresponds to 1.1 arc-second. Since the seeing will typically be noticeably worse than 1 arc-sec, focus accuracy amounting to about 1-2 seconds of motor motion at "dead slow" is appropriate.

8. Photometric calibration: The theory for transforming instrumental color index and magnitude to standard color index and magnitude is covered in references 1, 2, 3 and 6. Assume that the target and comparison stars are close enough to the calibrated standard stars that atmospheric effects (e.g. variation of transparency with zenith angle) can be neglected – meaning that the target star and the calibration field are within about 10 degrees of each other. Then, the general idea for differential photometry and colorimetry is to assume a linear relationship between the measured "instrumental" magnitude/color and the standard magnitude/color.

Using the following nomenclature:

b_{ADU}, v_{ADU}, r_{ADU} = the measured signal (ADU's) through the blue, visual, and red filters,

b_0, v_0, r_0 = "instrumental" magnitude in the blue, visual, and red filters (corrected for extinction to exo-atmospheric values using $b_0 = b - k_b \cdot X$ where X= air mass),

and

B, V, R = "standard" magnitude of the star in the blue, visual, and red filter bands,

The "instrumental" magnitudes observed in an image will be:

$$b = -2.5 \log (b_{ADU}) - k_b \cdot X$$
$$v = -2.5 \log (v_{ADU}) - k_v \cdot X$$
$$r = -2.5 \log (r_{ADU}) - k_r \cdot X$$

The conventional theory assumes that the "instrumental" color index is related to the "standard" color index by a linear equation.:

$$[B\text{-}V] = T_{bv} \cdot (b\text{-}v)_0 + Z_{bv}$$

and

$$[V\text{-}R] = T_{vr} \cdot (v\text{-}r)_0 + Z_{vr}$$

Starting with these model assumptions, a series of measurements are made on standard calibration stars (e.g. the Landolt fields), and the measured (b-v) is compared with the published (B-V). The conventional approach is to plot {[B-V] – (b-v)} against [B-V], and use a least-squares linear fit to compute the values of T_{bv} and Z_{bv}. Graphically, this conventional theory assumes that the plot for the standard stars will look like:

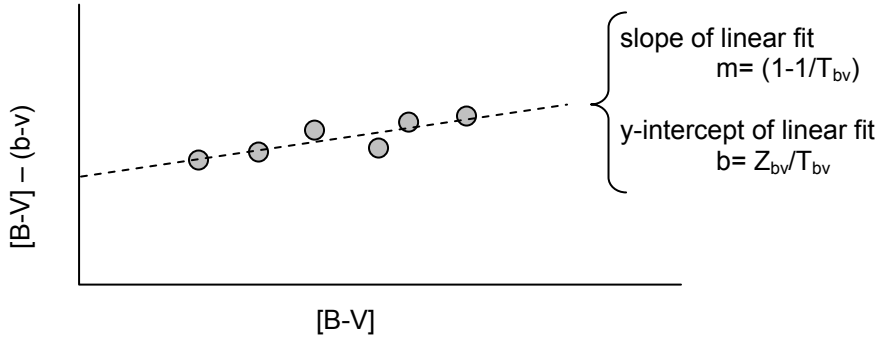

with a similar plot for [V-R] to find Tvr and Zvr.

Once the linear fit is determined using standard stars (e.g. Landolt standards), the coefficients can then used to transform the measured color index of any target star or asteroid to the standard color index. Note that if the instrument and filters are a good match to the standard photometric system, then the coefficients T_{bv} and T_{vr} will be approximately ≈ 1.0

The conventional theory continues by assuming that the measured instrumental v-band magnitude is related to the true V-magnitude by a linear function of color index. Using the (V-R) color index, we assume that:

$$(V\text{-}v_0) = T_{v,VR} * [V\text{-}R] + Z_{v,VR}$$

or, using the (B-V) color index, we assume that

$$(V\text{-}v_0) = T_{v,BV} * [B\text{-}V] + Z_{v,BV}$$

The zero-point coefficient ($Z_{v,bv}$ or $Z_{v,vr}$) is what transforms the data from the measurement units (i.e. log ADUs) to standard photometric (V-magnitude) units. If the instrument filters are a good match to the standard photometric filter passbands, then the coefficients $T_{v,BV}$ and $T_{v,VR}$ will be approximately ≈ 0.

Again, graphically, the conventional theory assumes that our plot of (V-v) against [B-V] or [V-R] for standard photometric reference stars will look like:

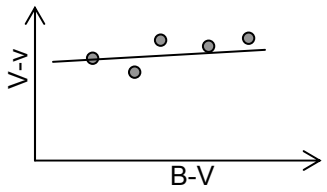

Once the coefficients have been determined by plotting and fitting to the data taken on a set of standard stars (e.g. Landolt fields), then the measured signal from a target object can be transformed into the standard passbands by the inverse equations:

$$V_{VR} = v_0 + T_{v,VR} * [V\text{-}R] + Z_{v,VR}$$

or

$$V_{BV} = v_0 + T_{v,BV} * [B\text{-}V] + Z_{v,BV}$$

Note that, based on the linearity study done above, the data collection for calibrating the color indices should be in the linear range of the CCD – i.e. integrated ADU signals of at least 10,000 ADUs are required.

8.1 B, V, R transformation constants: During 2004 I made several measurements of the transformation coefficients, in conjuction with asteroid light-curve studies. The results were quite consistent, with the following results:

Band or Index	Tranformation Coefficient	± 1-σ
B-V	T_{bv} = 1.437	0.11
V-R	T_{vr} = 1.068	0.03
V_{BV}	$T_{v,BV}$ = -0.05	0.02
V_{VR}	$T_{v,VR}$ = -0.066	0.035

A word about exposure length in all of these color and magnitude transformations: The trasnformation equations include "zero-point" values (e.g. $Z_{v,BV}$ and $Z_{v,VR}$). These are the numbers that translate "log ADU" into "magnitude", and hence the whole analysis presented above is based on the assumption that all data collected used the same CCD exposure duration. As a practical matter, the CCD is more sensitive in some bands than others (e.g. the B band sensitivity is nearly an order of magnitude less than R band). Hence, it will often be desirable to make longer exposures in B band (to achieve a staisfactory S/N ratio), and shorter exposures in R band (to avoid saturation). MPO Canopus/PhotoRed accounts for different exposure durations – it reports instrumental magnitude in each image, reduced to standard exposure length of 1 second.

8.2 Unfiltered characterization:
Of course, if only unfiltered observations are made, then the actual [B-V] and [V-R] color indices aren't known. For asteroid photometry, a reasonable first-approximation is to assume that the asteroid's spectrum matches the sunlight that it reflects. Solar-type stars' color indices are:

$$[B\text{-}V]_{Sun} = 0.674 \quad \text{and} \quad [V\text{-}R]_{Sun} = 0.505$$

A (probably better) assumption is that "typical" asteroid colors are (per Harris [ref 5]):

$$[B\text{-}V]_{asteroid} = 0.8 \quad \text{and} \quad [V\text{-}R]_{asteroid} = 0.4$$

The spreadsheet makes this assumption for converting unfiltered ADU's to V-magnitude. The curve below shows the approximate V-mag vs ADUs (again normalized to a 60 second exposure). This shows that a 60-second unfiltered exposre can get very good S/N ratio on targets as faint as mag 15.5. Longer exposures can go somewhat fainter, of course.

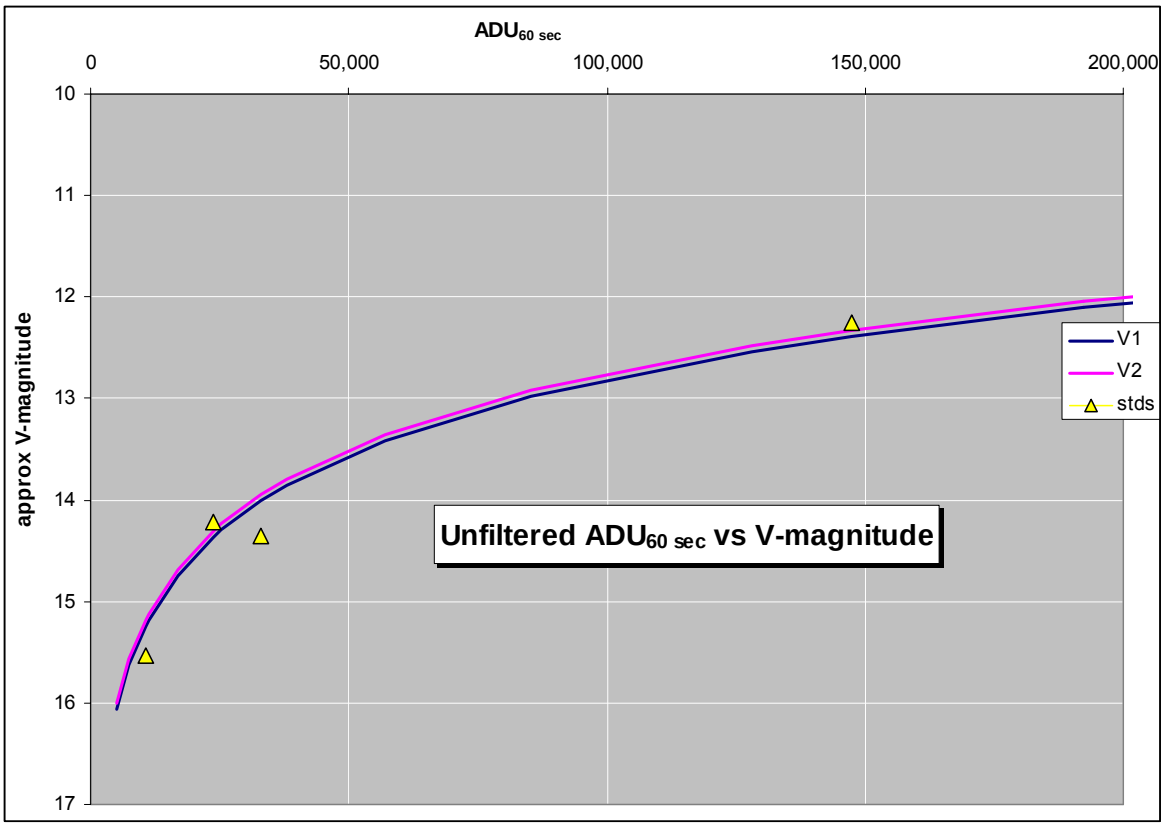

8.3 First-Order Extinction: During 2004 I made quite a few measurements of atmospheric extinction ("first-order" extinction), using both Comp-Star and Hardie methods of evaluation. The results for "typical clear nights" at Altimira Observatory were:

Band	avg. extinction (mag/air mass)	std dev
B	0.53	0.35
V	0.28	0.12
R	0.20	0.10

8.4 Second-order extinction: Second order extinction was determined by the standard method, as described in Henden & Kaitchuk (ref 6): a series of images in all three filters (B, V, R) were taken of a field containing a "blue" and a "red" star, covering a wide range of air mass. Call the "red" star #1, and the "blue" star #2: The relevant equations are:

$$(b\text{-}v)_{1,0} = (b\text{-}v)_1 - k'_{bv} X - k''_{bv} (b\text{-}v)_1 X$$

$$(b\text{-}v)_{2,0} = (b\text{-}v)_2 - k'_{bv} X - k''_{bv} (b\text{-}v)_2 X$$

Subtracting and rearranging gives

$$[(b\text{-}v)_{1,0} - (b\text{-}v)_{2,0}] = [(b\text{-}v)_1 - (b\text{-}v)_2] - k''_{bv} [(b\text{-}v)_1 - (b\text{-}v)_2]X$$

The term on the left is a constant, so this is a linear equation:

$$\Delta(b\text{-}v) = k''_{bv}\,[\Delta(b\text{-}v)]\,X + \text{const}$$

where

$$\Delta(b\text{-}v) = [(b\text{-}v)_1 - (b\text{-}v)_2]$$

so that plotting $\Delta(b\text{-}v)$ versus $[\Delta(b\text{-}v)]\,X$ should be a straight line, whose slope is the second-order extinction k''_{bv}. (A similar formulation can be used to check for k''_{vr}.)

The field containing HD50279 and HD50167, recommended in ref 6, and shown in the Figure below was used. This field fortuitiously contains two bright red-blue pairs

field center:
RA= 06:52:10.3
Dec= +01:07:00

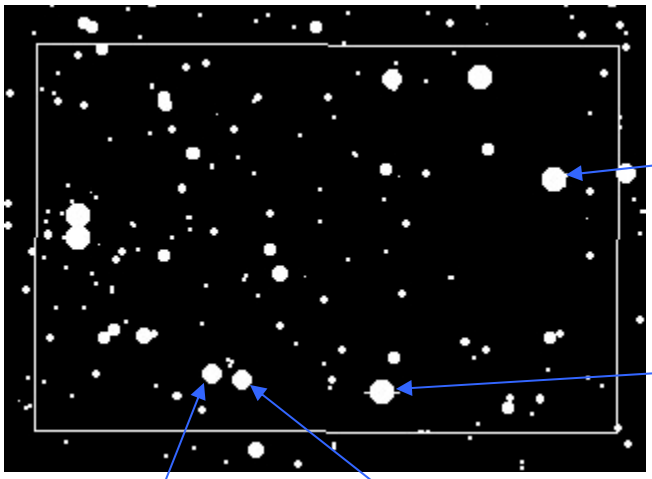

One night was devoted to a nearly-continuous image sequence of this field. The images were reduced in PhotoRed, using a 21-pixel diameter measuring aperture.

Two approaches were taken to data analysis: "conventional" and "line fitting".

The "conventional" approach is to match up B, V, and R images taken at nearly the same air mass, and treat them as having been taken at the same identical air mass. Plotting the two fields in this way gives:

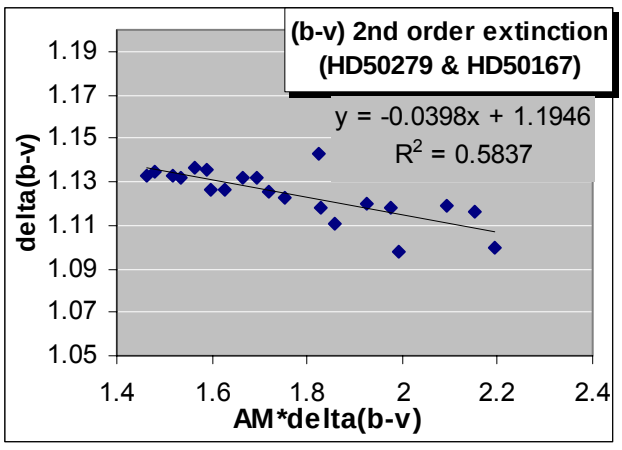

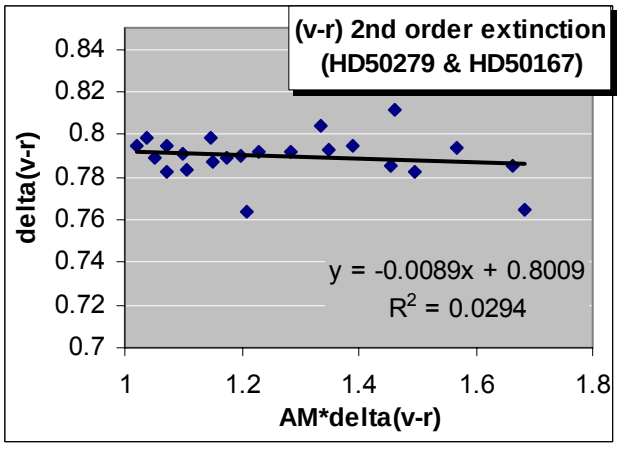

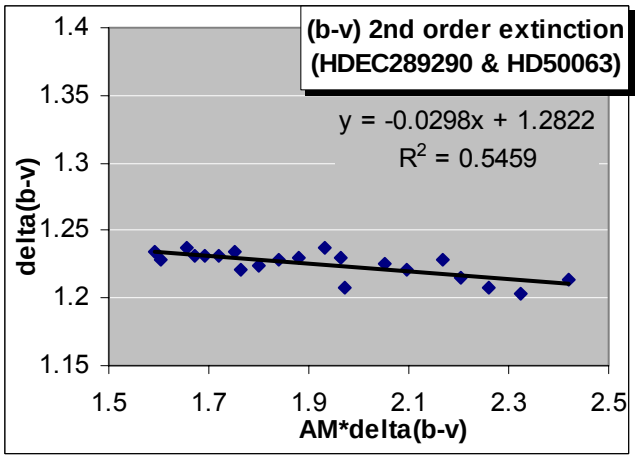

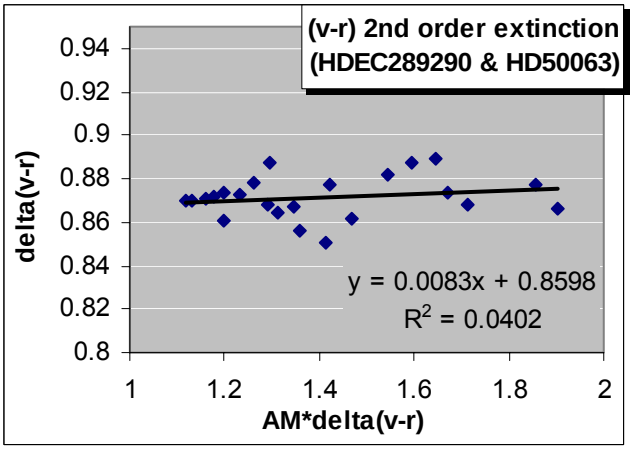

As a check as to whether the scatter in individual data points had a singificant effect on these results, a "line fitting" approach was also tried. The concept is to create a linear fit to the IM vs X for each star, and then use those fits as the basis for plotting Δ(b-v) vs Δ(b-v) X.

A typical linear fit (showing 1st order extinction in the b-band) is:

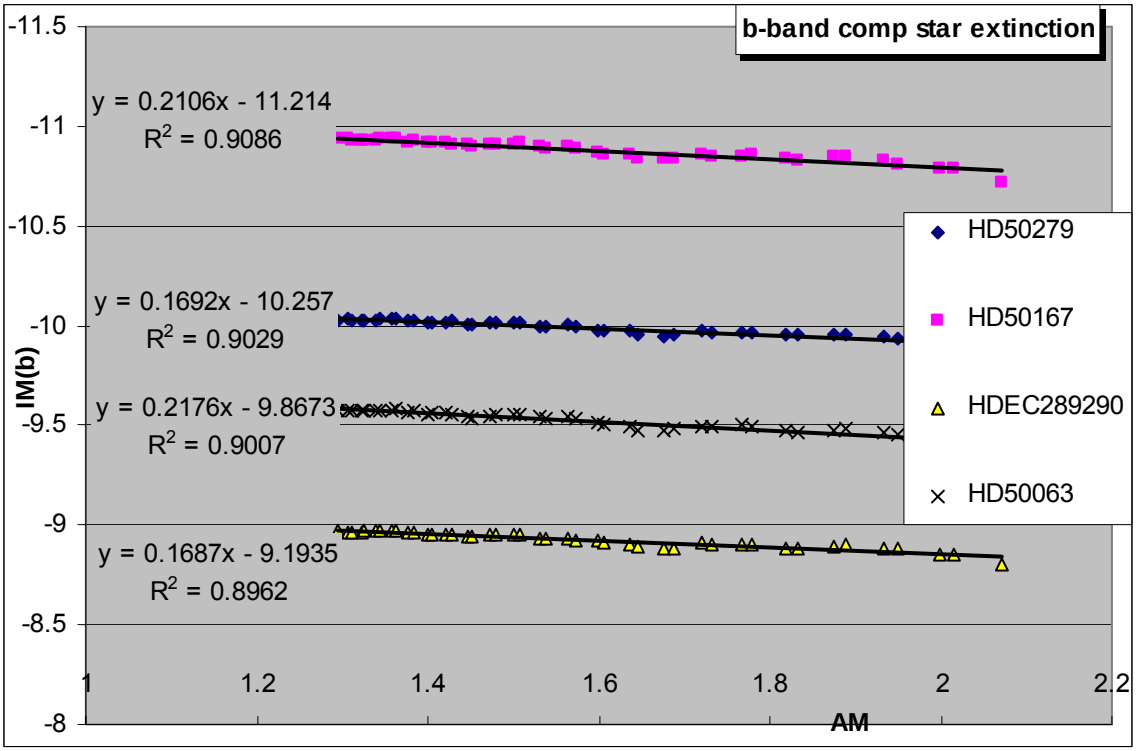

Using these linear fits (determined in all three colors) to determine the second-order extinction gives:

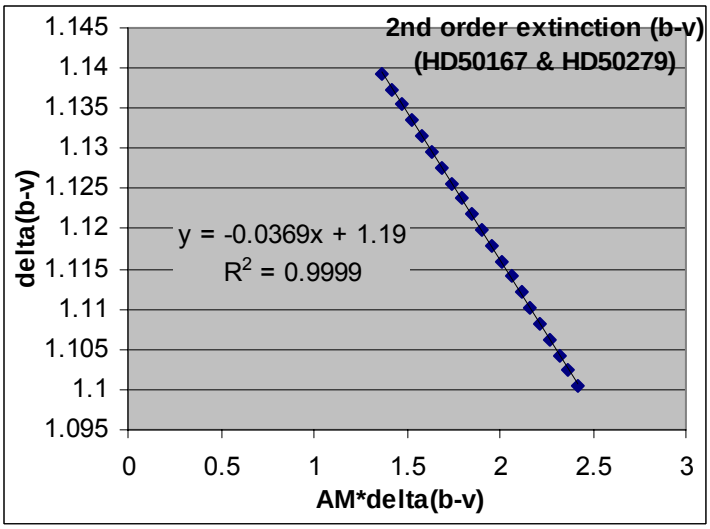

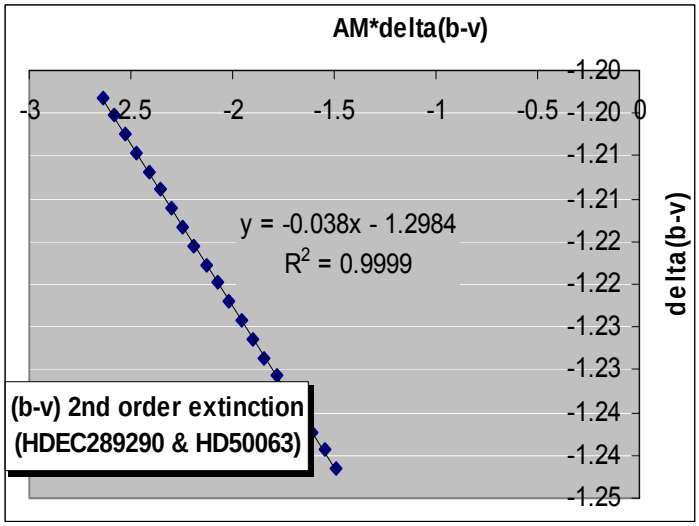

It is heartening that these two results are consistent with each other:

A summary of these results is shown in the Table below:

parameter	HDEC289290 & HD50063	HD50167 & HD50279
(b-v) 2nd order extinction:		
k''_{bv} using data points	-0.0298	-0.0389
k''_{bv} using linear fits	-0.038	-0.0369
(v-r) 2nd order extinction:		
k''_{vr} using data points	+0.0083	-0.0089
k''_{vr} using linear fits	+0.0014	-0.017

Based on these results, I'll use the global average for second order extinctions:

$k''_{bv} = -0.036$

$k''_{vr} = +0.004 \approx 0$

9. Typical Signal levels vs. stellar magnitude: It is handy to know approximately what exposure duration is required to reach a certain magnitude stellar object. A series of images were made on 9/5/03 of four standard stars (in field SA 113) at several exposure durations, to characterize the sensitivity of the imager in 3 B, V, and R filters, as well as unfiltered. These measurements were made on a "typical" night, and the results below are not corrected for extinction, nor for color index, so they represent "typical" conditions. (The standard stars used ranged from 0.519 < [B-V] < 1.344, and 0.34 < [V-R] <0.897). The graph below shows the observed signal levels, all normalized to a 60-second exposure:

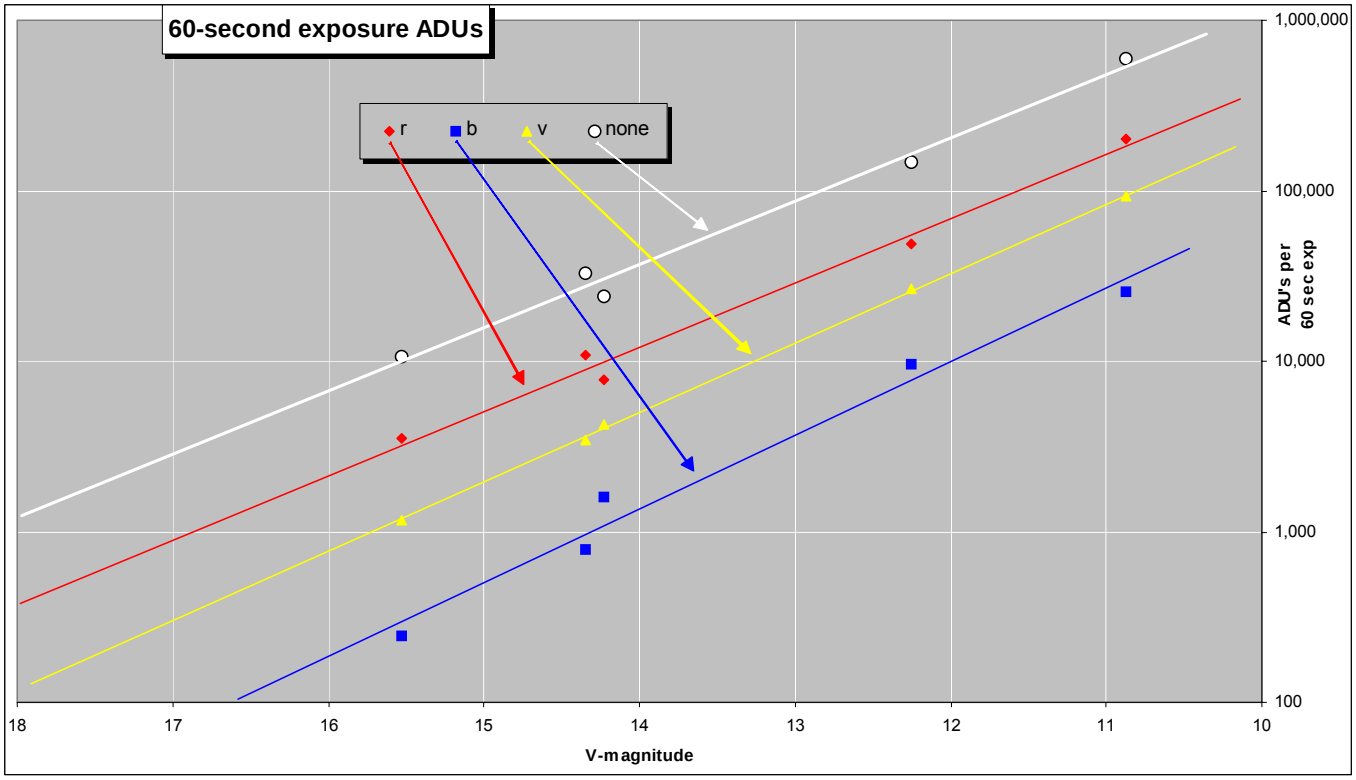

Note that the slopes of the trend lines are all very close to the (theoretical) 1/2.5 = 0.4. Figuring that SNR= 100:1 requires about 10,000 ADU signal level, good photometry can be done in V-band to about mag 13.5 with 1 minute exposure.

Another way to look at this data is to ask, "what exposure do I need in order to get a high SNR on a particular target?" The answer is shown in the figure below, which shows the exposure required to achieve SNR ~ 100:1, given the V-magnitude of the target. (Obviously, this assumes that the target color is in the range of "typcial" stellar colors).

For targets down to V= 14, a v-band exposure of 2 minutes should suffice. To get down to V= 15, a 6 minute v-band exposure, or a 3-minute r-band exposure is required.

Unfiltered 4-minute exposures should provide photometry down to almost V= 17th magnitude.

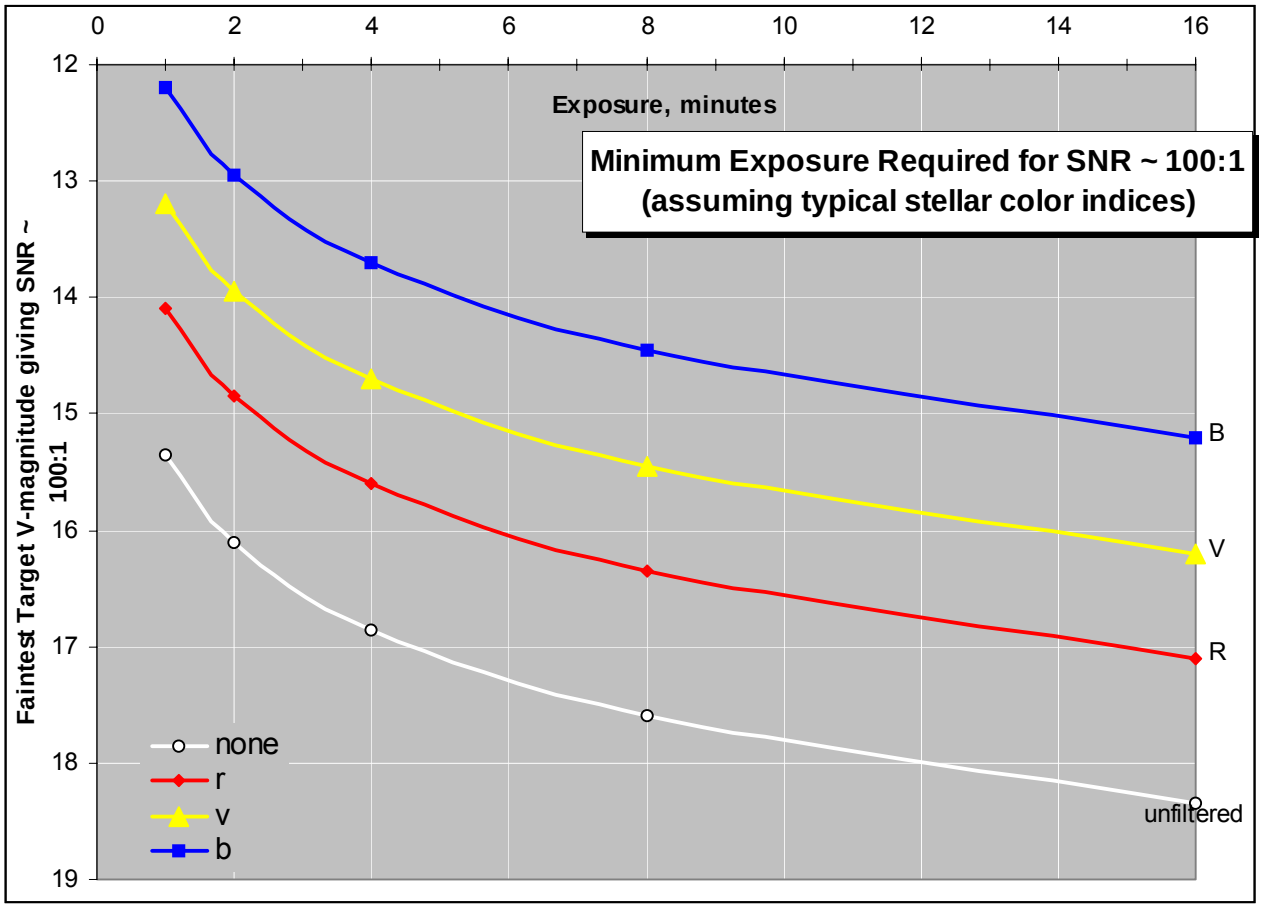

10. FITS header time-tag: Astrometric measurements require accurate time-tag of the image (and knowledge of what the time-tag in the FITS header means). Sequences of images , e.g. for asteroid light-curve photometry, have been known to suffer from timing errors because of the camera control software periodically stopping the PC clock. This series of characterizations investigated both of these effects.

10.1 Meaning of FITS header time tag: The FITS header time written by CCDOps is the UT of the *start* of the exposure.

This was checked by making several images ranging from 60 sec to 240 sec, and starting them from a WWV time-tick. During one "auto-grab" sequence, I also checked the actual start time of one exposure. In both of these checks, the time recorded on the FITS header matched the start of exposure to within ±3 sec. This deviation is probably human response error.

10.2: Stability of PC clock during imaging sequences: The normal nightly routine is to synchronize the PC clock to WWV at the start of each evening. During random checking in the course of a couple of nights, no significant errors were seen in the PC clock over a single night's run of nearly-continuous imaging (for photometric monitoring).

11. Miscellaneous performance baseline data: The purpose of these characterizations is to document "baseline" performance of the telescope operation when everything was new, as an aid in identifying any changes, wear, or shift; or for troubleshooting future malfunctions.

11.1 Polar alignment accuracy: It is of interest to confirm the accuracy of telescope polar alignment during drift-alignment. The misalignment will appear as field-of-view rotation in guided CCD images.

The derivation of drift-rate vs polar alignment error is given in the Figure below.

Using the reticle eyepiece with a 15 arc-sec reticle width, and a star at the celestial equator, the polar alignment error is:

$$\varepsilon = 0.95/(\Delta t) \text{ degrees}$$

where Δt is the niumber of minutes the star takes to drift across the reticle width (in declination).

Using the CCDOps auto-guide track file, the declination drift can be estimated by integrating the declination corrections. If the integrated correction is δ arc-sec in a session of t minutes, then the estimated polar alignment error is

$$\varepsilon = 57.3 * (4.8 * 10^{-6}) * \delta/(\omega t),$$

where the siderial rate is ω= .0044 rad/minute (for stars at the celestial equator) , giving

$$\varepsilon = 0.0625 * (\delta/t) \text{ degrees (with } \delta \text{ in arc-sec and t in minutes)}$$

This formula is convenient because the pixel size (with scope at f/6.3) is almost exactly 1 arc sec per pixel.

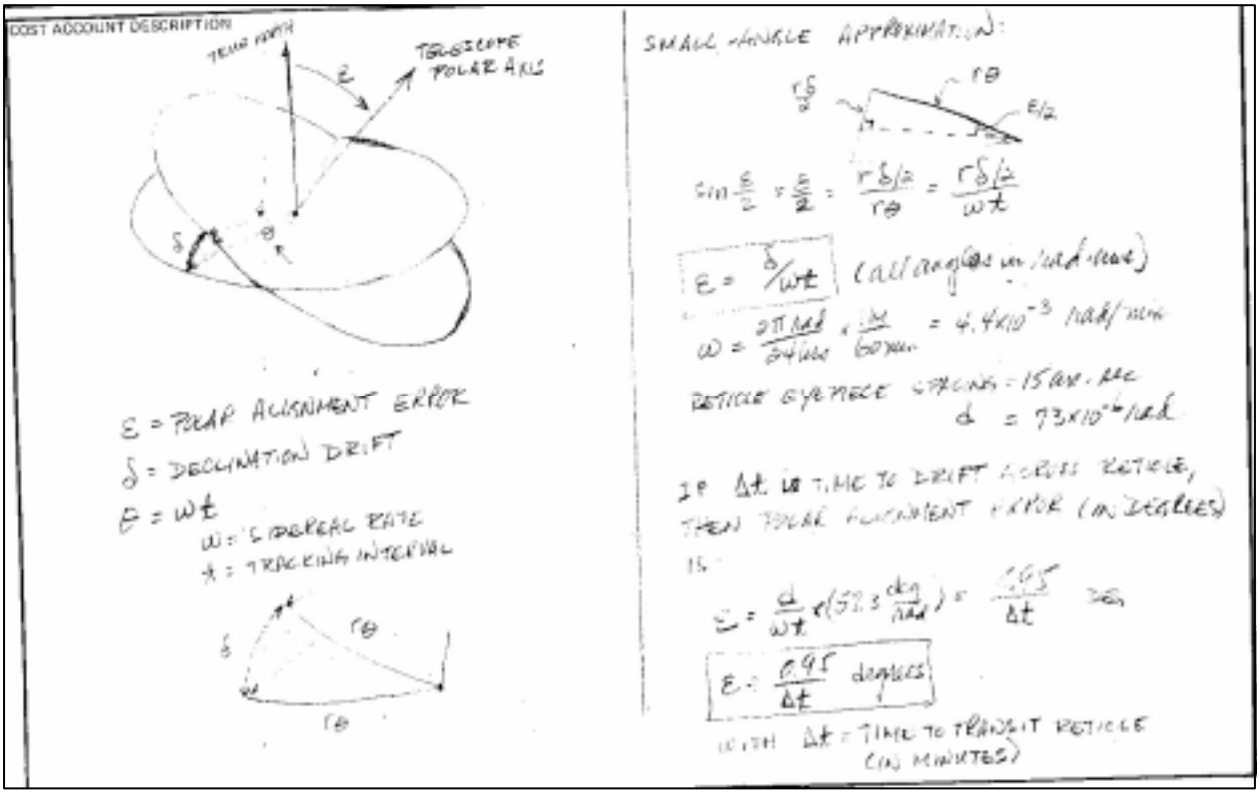

11.2 Achievable polar alignment accuracy: The pier mounting bolts are ¾" X 10 tpi, spaced about 12" apart, as shown in the sketch below. Assuming that the smallest controllable rotation of the nuts is ¼ turn, then the the best achievalbe polar alignment accuracy is:

$\varepsilon_{min} \approx \tan^{-1} [(¼) (1/10) / 12]$

$\varepsilon_{min} \approx 0.1$ degree

This will result in declination drift of about δ-dot ≈ .026 degrees per hour ≈ 94 arc-sec per hour.

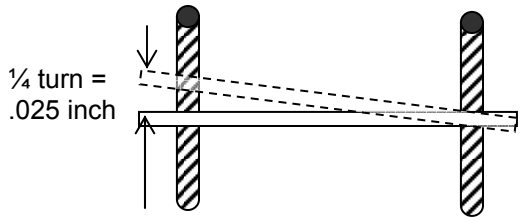

6. Tracking and Guiding

6.1 Typical Autoguide characteristics: In order to assess both tracking and polar alignment accuracy, auto-guide logs were recorded on YYYY-MM-DD ("active axes" = None in autoguide set-up). The conditions of the autoguide logs are descried in the following table:

Date of observations		10/14/03	
Target star		unk, near culmination at celestial equator	
Target star magnitude		approx mag 5	
Autoguide conditions:			
exposure		2 sec	
filter		V	
guide star S/N ratio		unk (high)	
Autoguide rates (calibration)		rate (pixels/sec)	at angle (deg)
	+X	7.7	182
	-X	7.3	2
	+Y	4.7	98
	-Y	4.6	297
max move=		2 sec	
autoguide using:		camera relays	
simultaneous X and Y relay action		checked (active)	

6.2 Telescope Tracking error: On October 13-14 2003 I made three tracking logs using the ST-8XE camera's autoguide capability, with both axes "inactive", to record the telescope's unguided tracking error. The results show pretty good polar alignment (i.e. very small errors in the Y-axis (Declination), but surprisingly poor tracking in RA.

6.2.1 Without PEC: The baseline tracking accuracy is based on unguided tracking of a bright (about mag 6) star on the celestial equator, and near its culmination. The plot below shows the results. (This was done using the autoguider chip, so 1 pixel ≈ 0.9 arc second).

The plot clearly shows the 8-minute period of the work gear, and a peak-to-peak tracking error of over 30 arc-seconds. The maximum error rate (which gives an indication of the correction rate that will be required of the autoguider) is nearly 1 arc-second per second. Typical

well-focussed stars in the main imager (on nights of good seeing) have FWHM ≈ 2.5 to 3 pixels (at 1.1 arc-sec per pixel), so in order to avoid noticeable trailing, it is desirable for the autoguid exposure and correction interval to be only 1 or 2 seconds.

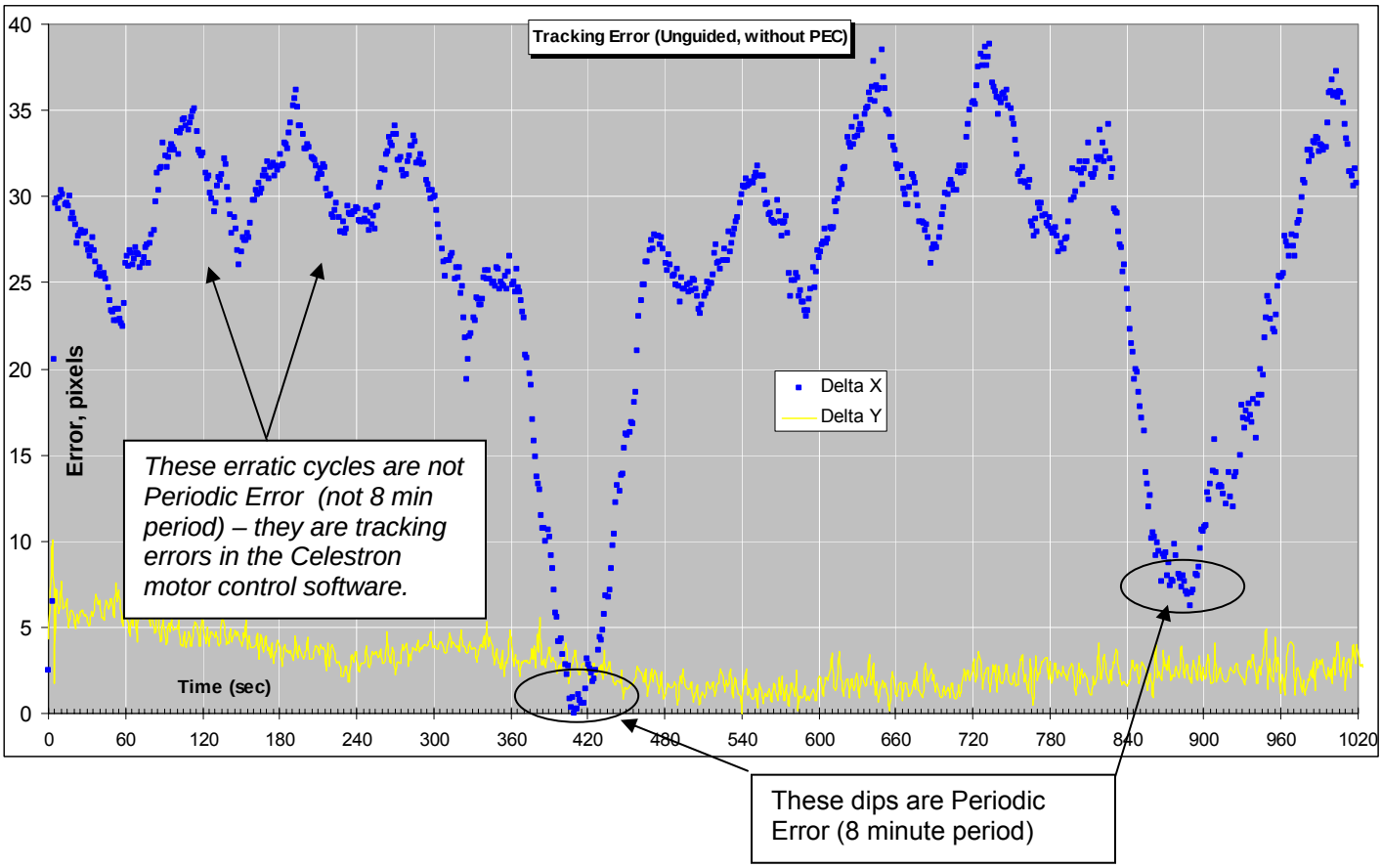

6.2.2 With PEC: The PEC was recorded by manual guiding using the reticle eyepiece and a 2X barlow. During this PEC training session, the star never went outside of the reticle center-box, so the peak-to-peak residual error should be no more than 8 arc-seconds. Following PEC training, the telescope tracking error was recorded as above, with PEC active. The results are shown in the graph below:

Because of the significant non-periodic error generated by the Celestron motor control software (per Lenny Schaffer and others on the NexStar Yahoo group), PEC is of no value. Until improved motor control software is released, active guiding is required for any exposure longer than a few seconds. (Note: upgrading to MC version 40.40 did not noticeably improve this situation.)

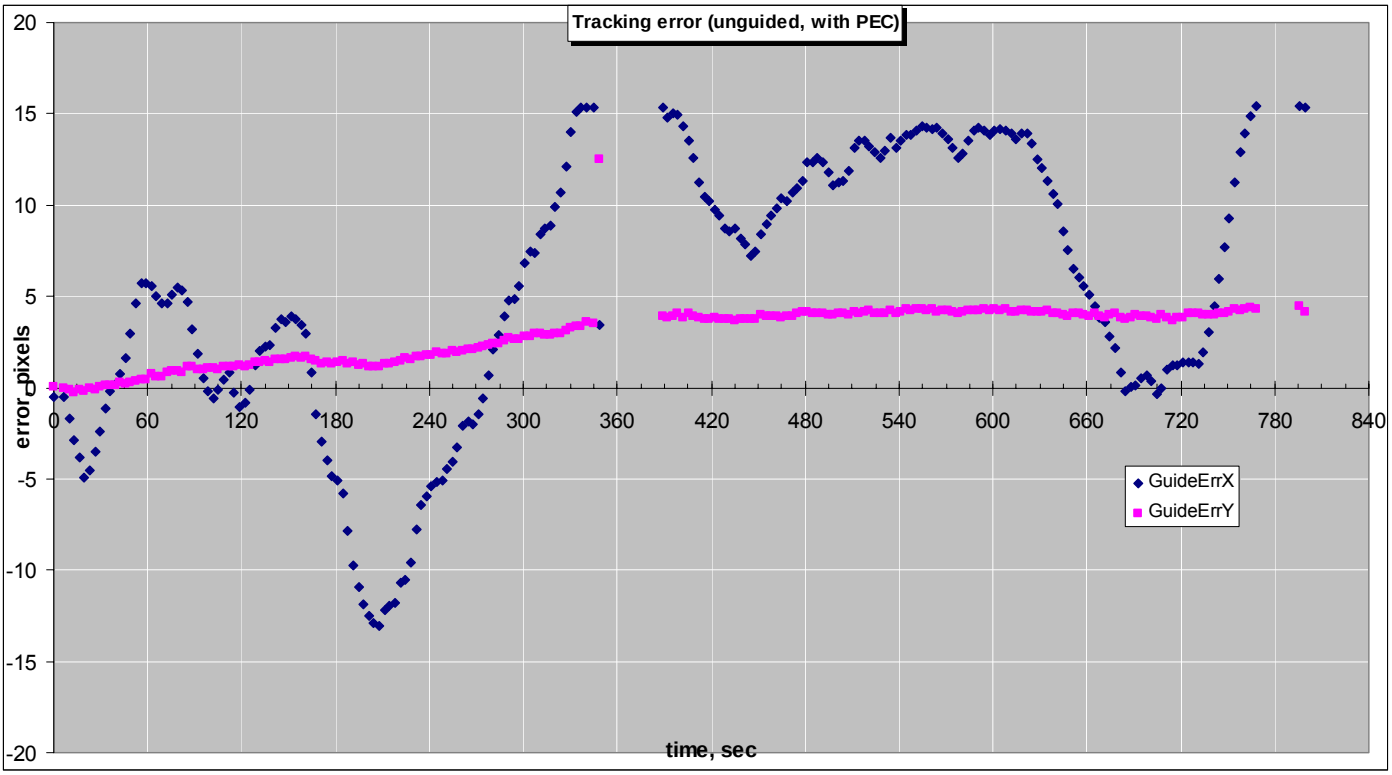

11.3 Software Settings: The following software settings have been updated to the configuraiton in Altimira Observatory:

11.3.1 CCDOps: CCD Ops Preferences are set to "use GMT in Image Header". This apparently reads the PC clock and setting (to pacific time) to establish the GMT offset. It has been checked and is correct.

11.3.2 CCDSoft: CCDSoft Preferences are set to "use GMT in Image Header", and "save files as FITS". PC clock should remain set to Pacific Time – the CCDSoft processing puts the correct GMT time in the FITS header

For autoguiding: the "reverse X" checkbox depends on camera orientation:

orientation	"reverse X"
cables down	uncheck
cables up	check

11.3.3 MPO Canopus: File/Settings have been updated to the following:

TAB				*references*
GENERAL				
Profile	Altimira Observatory			
Longitude	-117:34:55	Latitude	+33:35:31	
Elev (m)	183			
UT offset	00:00:00			
FL (m)	69.30	e/ADU	2.3	*per SBIG manual*

Col (pix)	1530	Size (µm)	9.0	
Rows (pix)	1020	Size (µm)	9.0	
Header exposure time =		START		
MPC				
COD	G76	ID 1	BND V	
TYP	Unidentified	COM	(blank)	
CON1	R. K. Buchheim, 18 Altimira, Coto de Caza CA 92679 USA			
CON2	[rbuchheim@compuserve.com]			
OBS	R. K. Buchheim			
MEA	R. K. Buchheim			
TEL	0.28-m f/6.3 schmidt-cassegrain + CCD			
NET	USNO A2.0			
ACK	Your astrometry report was recieved			
AC2	(blank)			
TO:	mpc@cfa.harvard.edu			
	NEW MPC format:	not checked		
CATALOGS				
√	MPOSC			
√	USNO			*all others unchecked*
CHARTING				*(used defaults)*
PHOTOMETRY				
	Default filter	V		
	Photometry Magnitudes	Instrumental		

11.4. Equipment References:

11.5. NexStar Telescope firmware versions:

		Motor Control		*notes*
Firmware	Hand Control	Az	Alt	
	2.2	40.40	40.40	*upgraded from MC v 4.3 3/26/04*
	GPS	Serial Bus		
	2.2	2.2		

NexStar telescope User-defined settings:
Anti-backlash: Az: Pos = 0, Neg=0
Alt: Pos = 26, Neg = 26

11.6 Electrical wiring in Observatory: Observatory power is all on house circuit breaker labeled "Lites".

11.7 Telescope balance positions for counterweights: Follow below diagrams:

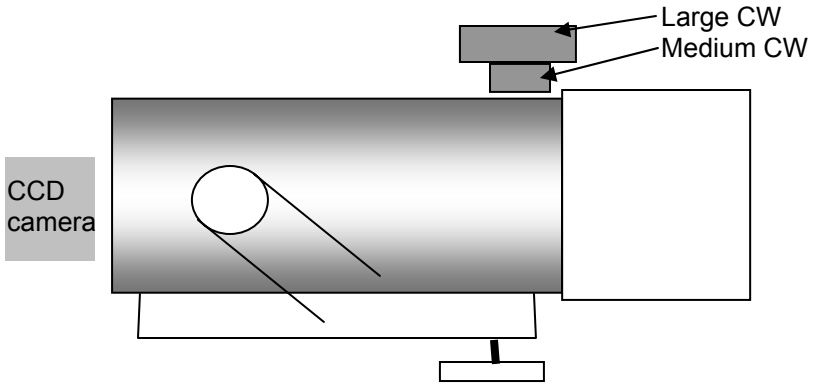

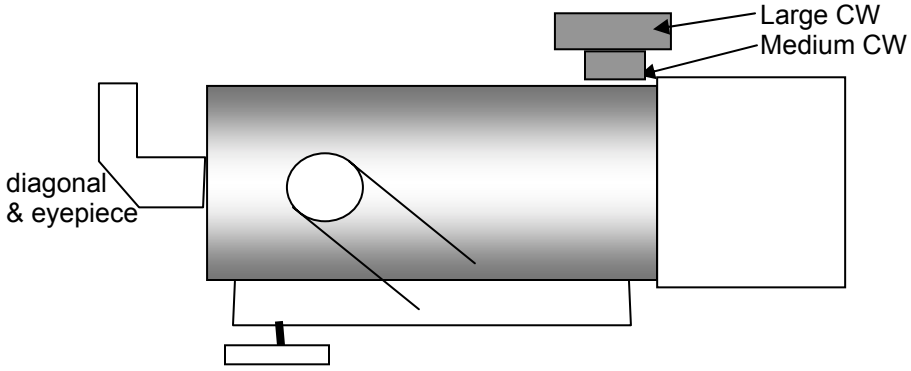

11.8 Filter positions in filter wheel: Per below sketch

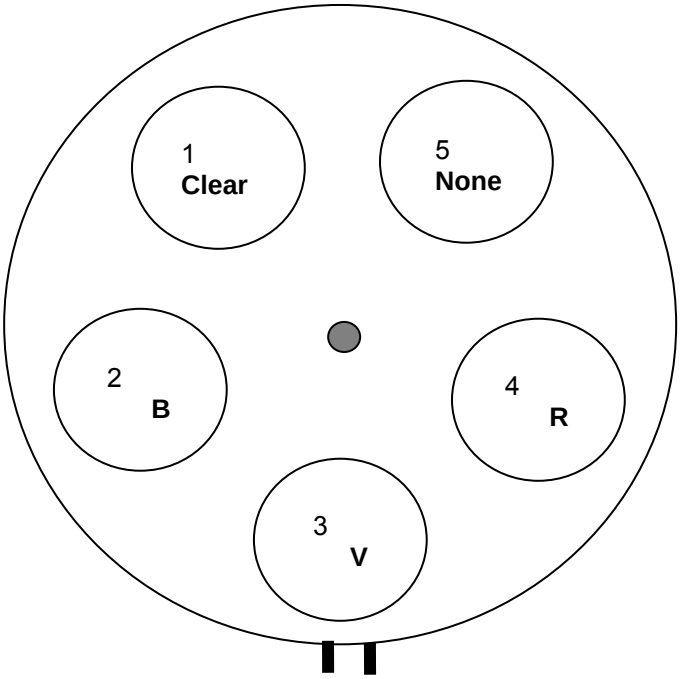

Filter positions in CCDSoft "Settings" command:

position	Filter
1	Clear
2	phot B
3	phot V
4	phot R
5	none

When using CCDSoft's "Color" tab to take mulit-filter sequences of images, the filter definitions entered into CCDSoft are:
"Red" --> red (Johnson-Cousins R)
"Green" --> visible (Johnson-Cousins V)
"Blue" --> blud (Johnson-Cousins B)

11.9 Automadome Calibration and Geometry
Dome Calibration = 114 motor turns per dome rotation
Dome/Telescope Geometry entered into Automadome:

Parameter	meaning	units	value	memo
Phi	latitude	radians	0.5863	= 33.59 degrees
Rdome	radius of dome	inches	45	
Xm, Ym, Zm	offset of mount	inches	+1.5, -6.5, -6	measured mount offset
Xt, Yt	telescope offset on mount	inches	0, 0	= fork-mounted scope
Yo	optical axis offset	inches	0	
ta, tb	telescope pointing angles	radians		used to check dome sync

Parameters (ta, tb) are in radians, used to confirm proper alignment of the dome. Ta = hour angle (=0 due south, increases counterclockwise, so 90 deg = 1.57 rad = due East)

Dome Azimuth is measured clockwise from North:

due North = 0
due East = 90 deg = 1.57 radians
due South = 180 deg = 3.14 radians
due West = 270 deg = 4.712 radians

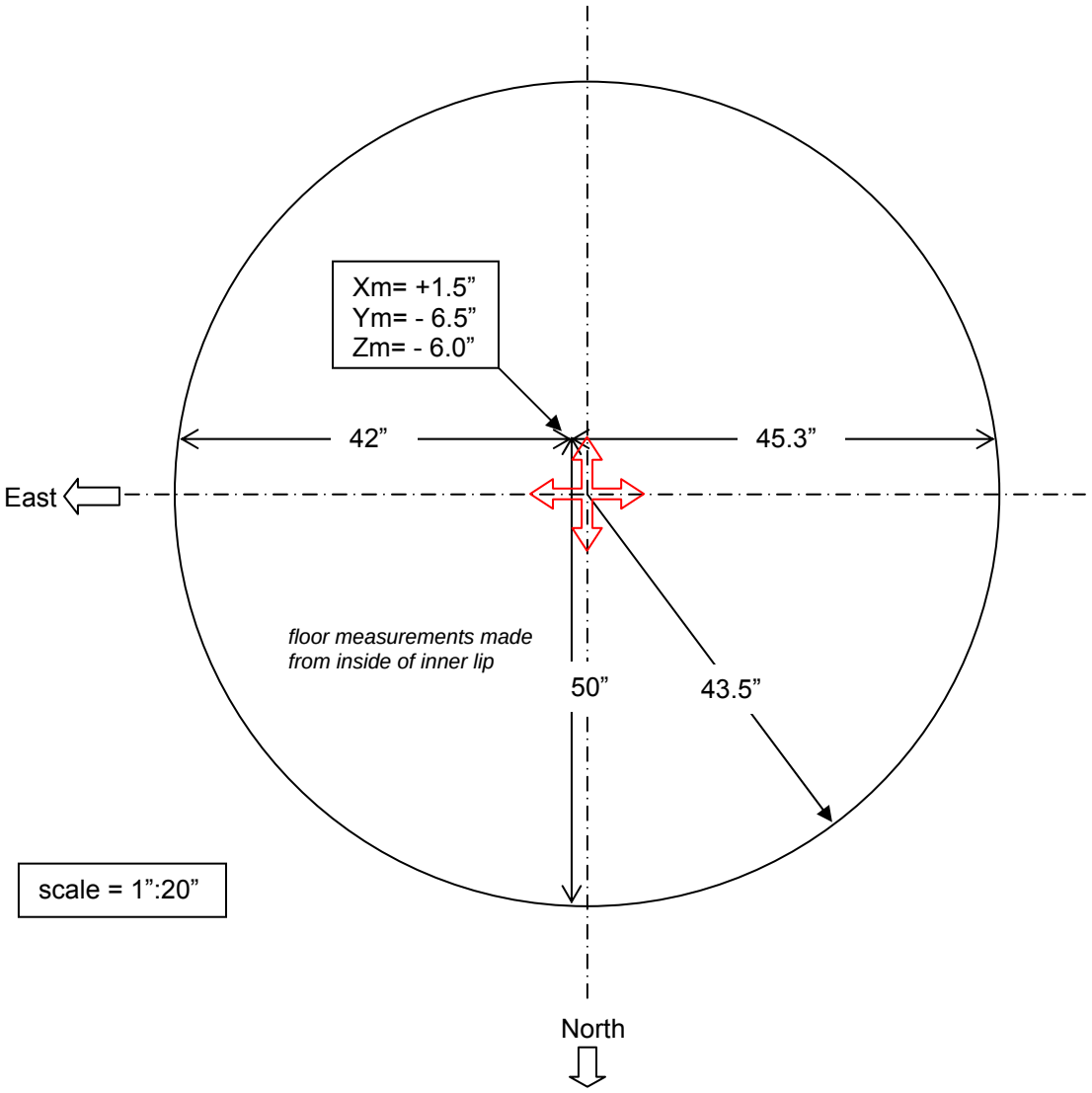

11.10: Wiring of Dome Motor to solar panel:

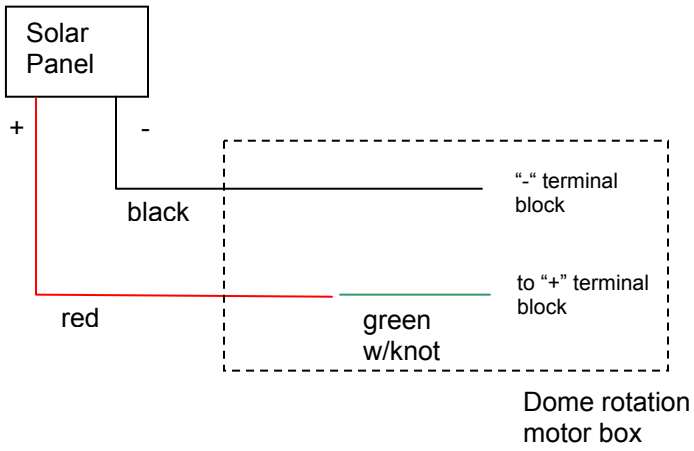

11. References:

1: Benson, Priscilla (C-Chair, AAVSO CCD committee) "CCD Trasnformation Coefficients", from AAVSO web site.

2. Zissell, "History of the Stellar magnitude System", from JAAVSO Vol 26, 1998, available fro AAVSO web site.

3. Hendon, A, "CCD Photometry" briefing charts (source unknown)

4. Smith, Paul S. "Standard Star Fields for UBVRI Photometric Calibration", (available at http://james.as.arizona.edu/~psmith/atlasinfo.html)

5. Harris, Alan, unpublished e-mail on MPML 24 Sept 1998.

6. Henden, Arne, and Kaitchuck, Ronald: Astronomical Photometry, 1990, Willmann-Bell, Richmond VA